

THE TEMPERATURE EFFECT OF POSITRON

ANNIHILATION IN ARGON

by

DOUGLAS BURTON MILLER

B.A.Sc., University of British Columbia, 1965

A THESIS SUBMITTED IN PARTIAL FULFILMENT OF

THE REQUIREMENTS FOR THE DEGREE OF

MASTER OF APPLIED SCIENCE

in the Department

of

PHYSICS

We accept this thesis as conforming to the
required standard

THE UNIVERSITY OF BRITISH COLUMBIA

February, 1968

In presenting this thesis in partial fulfilment of the requirements for an advanced degree at the University of British Columbia, I agree that the Library shall make it freely available for reference and study. I further agree that permission for extensive copying of this thesis for scholarly purposes may be granted by the Head of my Department or by his representatives. It is understood that copying or publication of this thesis for financial gain shall not be allowed without my written permission.

Department of Physics

The University of British Columbia
Vancouver 8, Canada

Date February 10, 1968

ABSTRACT

Lifetime techniques have been used to measure the direct annihilation rate in Argon gas as a function of temperature. In order to accomplish this, a pressure chamber capable of holding 10 amagats of gas at 300°C was designed and constructed.

The temperature of the Argon gas was varied between 140°K and 480°K. The results were collected at specific temperatures for gas densities of 8.0 and 10.2 amagats. The direct annihilation rate was found to be a decreasing function of temperature meaning it is a decreasing function of velocity. The direct annihilation rate decreased by 30% over the range investigated. Various functions in temperature were fitted to the results by the least squares technique.

The shoulder width-density product was found to be constant with temperature indicating that the shoulder annihilations take place at velocities significantly greater than thermal velocities.

The statistics on the ortho-positronium lifetime were not sufficiently good to see a temperature variation of this component.

A comparison of an electric result with these results gave a position - Argon atom scattering rate of $9.0 \times 10^{11} \text{ sec}^{-1} \text{ am}^{-1}$. This was assuming that the scattering rate was independent of velocity.

TABLE OF CONTENTS

| | <u>Page</u> |
|---|-------------|
| CHAPTER I INTRODUCTION | 1 |
| A. Annihilation in Gases | 2 |
| B. The Annihilation Time Spectrum | 3 |
| C. Discussion of Velocity Effects on Positron Annihilation in Argon | 5 |
| D. Discussion of Velocity Effects on Positron Annihilation in Helium | 7 |
| E. The Justification for Temperature Experiments | 8 |
| CHAPTER II THE CHAMBER | 10 |
| A. The Design Criterion | 10 |
| B. The Completed Chamber | 11 |
| C. The Choice of Material | 12 |
| D. The Shape and Size of the Chamber | 14 |
| E. The Number of Positrons Lost in the Walls | 15 |
| F. Gamma-Ray Attenuation | 16 |
| G. The Calculation of the Strength of the Chamber | 17 |
| 1) Cylindrical Walls | 18 |
| 2) Bottom Plate | 18 |
| 3) Top Plate | 19 |
| 4) Radial Stress in Flange | 20 |
| 5) Longitudinal Stress in Flange | 21 |
| 6) Exterior Plumbing | 21 |
| 7) Bolt Load | 22 |

| | |
|--|----|
| H. The Pressure Test of the Chamber | 22 |
| I. The Electric Field Grid | 23 |
| CHAPTER III EXPERIMENTAL DETAILS | 24 |
| A. The Experimental Set-up of the Electronics. | 24 |
| B. The Preparation of the Chamber for Temperature Variation | 25 |
| 1) High Temperature Set-up | 26 |
| 2) Low Temperature Set-up | 26 |
| C. The Gas Filling | 27 |
| CHAPTER IV PRESENTATION OF RESULTS | 29 |
| A. The Scope of the Results | 29 |
| B. The Analysis of the Time Spectra | 29 |
| C. The Results | 30 |
| D. The Interpretation of the Results | 31 |
| 1) The Temperature Dependence of the Direct Annihilation Rate, λ_a . | 31 |
| 2) The Temperature Dependence of the Ortho- positronium Annihilation Rate, λ_o . | 33 |
| 3) The Dependence of the Direct Rate on Density | 33 |
| 4) The Density Dependence of the Orthopositronium Annihilation Rate. | 34 |
| 5) The Shoulder Width | 35 |
| E. Calculation of the Direct Annihilation Cross-Section from the Results of the Least Squares Curve Fitting | 36 |

| | |
|---|----|
| F. Calculation of the Scattering Cross Section | 40 |
| G. Estimation of Errors | 41 |
| CHAPTER V CONCLUSIONS | 43 |
| BIBLIOGRAPHY | 44 |
| APPENDIX CALCULATION OF THE LONGITUDINAL STRESS IN THE FLANGE OF THE CHAMBER | 46 |

LIST OF TABLES

| | Page |
|---|-----------------------|
| I. Ultimate Tensile Strengths at Different Temperatures | 12 |
| II. Strength and Ductility of Stainless Steel at 298°K and 77°K. | 13 |
| III. Coefficient k for Equation 114 of Timoshenko (1956) | 19 |
| | <u>To follow page</u> |
| IV. Results from the Maximum Likelihood Fitting | 30 |
| V. Results of Fitting λ_a/D versus T by Least Squares. | 32 |
| VI. Results of Fitting λ_o versus T by Least Squares. | 33 |
| VII. Results of Fitting λ_a versus D by Least Squares. | 34 |
| VIII. Results of Fitting λ_o versus D by Least Squares. | 34 |

LIST OF FIGURES

| | <u>To follow page</u> |
|---|-----------------------|
| 1. A Typical Time Spectrum | 3 |
| 2. Electric Field Results (Orth, 1966). | 6 |
| 3. The Chamber | 11 |
| 4. Uniform Load on a Circular Flat Plate with Hole and Freely Supported Edges. | 19 |
| 5. Inner Circle Load on a Circular Flat Plate with Hole and Freely Supported Edges. | 19 |
| 6. A Block Diagram of the Electronics Used | 24 |
| 7. Integral Linearity of the Time Sorter | 24 |
| 8. Differential Linearity of the Time Sorter | 24 |
| 9. The Low Temperature Configuration | 26 |
| 10. A Graph of the Direct Annihilation Rate per Amagat, λ_D/D , Plotted Against Temperature, T. | 31 |
| 11. A Graph of the Ortho-Positronium Annihilation Rate, λ_o , Plotted Against Temperature, T. | 33 |
| 12. A Graph of the Direct Annihilation Rate, λ_D , Plotted Against Density, D. | 34 |
| 13. A Graph of the Ortho-Positronium Annihilation Rate, λ_o , Plotted against Density, D. | 34 |
| 14. A Diagram Showing Forces and Moments on the Flange. | 46 |

ACKNOWLEDGEMENTS

I wish to thank my supervisor, Dr. G. Jones, for accepting me as a student and suggesting the topic of my investigation.

I wish to thank Dr. P.H.R. Orth for his assistance during the experiment.

I wish to thank D. Stonebridge and P. Haas for building the chamber and other apparatus used during the experiment.

Finally, I wish to thank the National Research Council of Canada for a Bursary and a Studentship held during this work.

CHAPTER I

INTRODUCTION

The positron was the first anti-particle to be discovered. It was observed in a cloud chamber track by Anderson in 1932. Since that time, the study of positron-electron annihilations has become very important, both experimentally and theoretically.

When an electron-positron pair annihilate, at least two photons must be produced in order to conserve momentum, spin, and energy. However, in very special cases, a positron can annihilate with an electron in the neighbourhood of an atom to produce only one photon, since the atom receives the excess momentum which the additional photon(s) would have carried off. The most common number of photons emitted in an annihilation event is two or three. Two photons are emitted if the spins of the positron and electron are aligned in opposite directions in space; that is, the total angular momentum is zero. Three photons are emitted when the spins of the positron and electron are in the same direction, making the total angular momentum equal to one. Annihilation by two photons is far more likely than annihilation by three photons (Deutsch, 1953).

A. Annihilation in Gases

The detailed explanation of the mechanisms for positron-electron annihilation in gases has been given by Falk (1965) and Orth (1966). Only a brief summary of these processes will be given here.

A large fraction of the positrons emitted by a positron source (e.g. Na^{22}) into a noble gas annihilate by direct annihilations. These occur between a positron and an atomic electron. Another large percentage of positrons annihilate by the mechanism of positronium formation. A low energy positron captures an electron from an atom forming a hydrogen-like atom called positronium which subsequently decays by annihilation. An unknown, but probably small proportion of the emitted positrons forms molecular complexes with the gas atoms. These complexes eventually decay when the positron annihilates with one of the atomic electrons. In addition, a fraction of the positrons annihilate in the walls of the chamber used to contain the gas. This fraction depends on the gas pressure and the dimensions of the chamber. Finally, a small number of positrons will annihilate in the source and source holder.

B. The Annihilation Time Spectrum

A typical time spectrum for the annihilation of positrons in inert gases is shown in Figure 1. The maximum in the time spectrum occurs at zero time and is called the prompt peak. This peak is due to annihilations in the walls of the chamber, in the source, and of para-positronium. The number of positrons annihilating in the walls of the chamber depends on the chamber size and the gas density (Celitans and Green, 1963). In an ideal experiment, this number would be zero. Para-positronium is a positronium atom with the spins of the electron and positron aligned in opposite directions. This atom annihilates very quickly into two photons with a lifetime of 0.125 n sec. These events are found in the prompt peak because all positronium is formed very early in time. That is, positronium is formed when the Na_{22} positrons have slowed to the 8-20 ev. energy region within a few nanoseconds (Tao, etal, 1963).

The next prominent feature in the time spectrum is the shoulder. All of the inert gases exhibit this phenonemum, except possibly Helium. The shoulder has been well documented by Tao etal (1963), Paul (1964), and Falk and Jones (1964). It is a part of the direct component which occurs from the annihilation of free positrons with atomic electrons in the

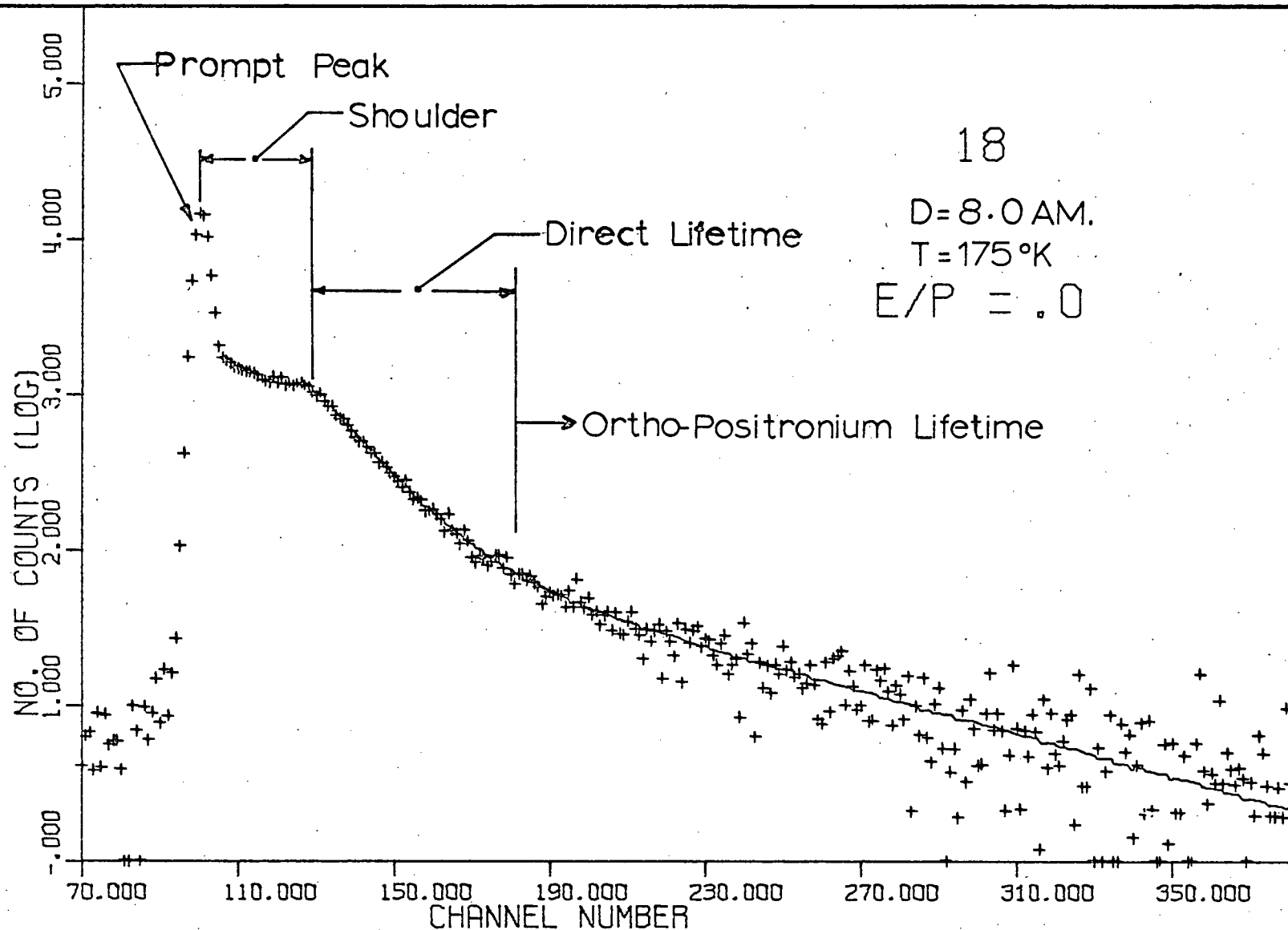


Figure 1: A Typical Time Spectrum.

inert gases The shoulder has been interpreted as the time spectrum of positrons slowing down by elastic collisions with the gas atoms from positronium formation threshold energies of 8-20 ev. to thermal velocities (Falk and Jones, 1964). The positronium formation threshold energy is that energy below which no positronium is formed. The existence of a shoulder indicates that the direct annihilation rate of positrons is velocity dependent.

Following the shoulder is the exponential component representing the direct lifetime of free thermalized positrons in the gas. This gives a constant rate of annihilation since an equal number of positrons are being scattered into high velocities as are being scattered into low velocities, rather than the excess of the latter events at velocities greater than equilibrium velocities. This process gives a constant rate despite the fact that the annihilation rate is dependent on velocity.

Further evidence that the annihilation rate in positrons in noble gases is velocity dependent is obtained by applying an electric field to the gas. The field accelerates the positrons to equilibrium velocities above thermal velocities. The results of Falk et al (1965) indicate that the annihilation rate in Argon is reduced when an electric field is applied.

In fact, if a reasonably strong field is applied, the positron energies are raised sufficiently to cause increased positronium formation.

The long lived component in the time spectrum (Figure 1) is caused by the decay of positronium atoms where the spins of the positron and electron are in the same direction. Such an atom is called ortho-positronium. Some of these ortho-positronium atoms decay by three-photon emission while others are "quenched" by colliding with gas atoms and decay by two-photon emissions. An electric field does not have an effect on the lifetime of this component (Orth, 1966). This is expected since the positronium atom is uncharged.

C. Discussion of Velocity Effects on Positron Annihilation in Argon

The time spectrum described in the last section has been used to obtain results for the annihilation rate of positrons in gases. The latest experimental results are those collected by Orth (1966) in Argon. The width of the shoulder multiplied by the gas density was observed to be 340 nsec-amagat, where an amagat is the density of the gas expressed in terms of atmospheres at 0°C. The shoulder width-density product appeared to be constant at different densities. This indicated that the interpretation of the shoulder as being the slowing down part of the direct lifetime component has some validity

in these experiments. When an electric field was applied to the gas in question, it was found that the shoulder width decreased until it disappeared altogether at high fields.

The direct annihilation rate, λ_a , was found to vary linearly with density, D , with a slope of $\lambda_a/D = (5.6 \pm 0.1) \times 10^6 \text{ sec}^{-1} \text{ am}^{-1}$.

The electric field dependence of the direct annihilation rate in Argon is shown in Figure 2 (Orth, 1966). It is to be noted that the annihilation rate per amagat decreases as the electric field, and hence the positron velocity, is increased. The annihilation rate per amagat starts to increase again at 90 volts $\text{cm}^{-1} \text{ am}^{-1}$ because of the increased positronium formation prevalent at this and higher fields. These results give a good qualitative indication of the annihilation rate's dependence on velocity. However, they do not define the velocity dependence of the annihilation rate because the elastic collision cross-section for the Argon-positron system is not known. If, instead, the temperature of the host gas is varied, the average positron velocity defined by the temperature of the gas will vary, and a more definite picture of the direct annihilation rate will emerge. This thesis describes such an experiment in which

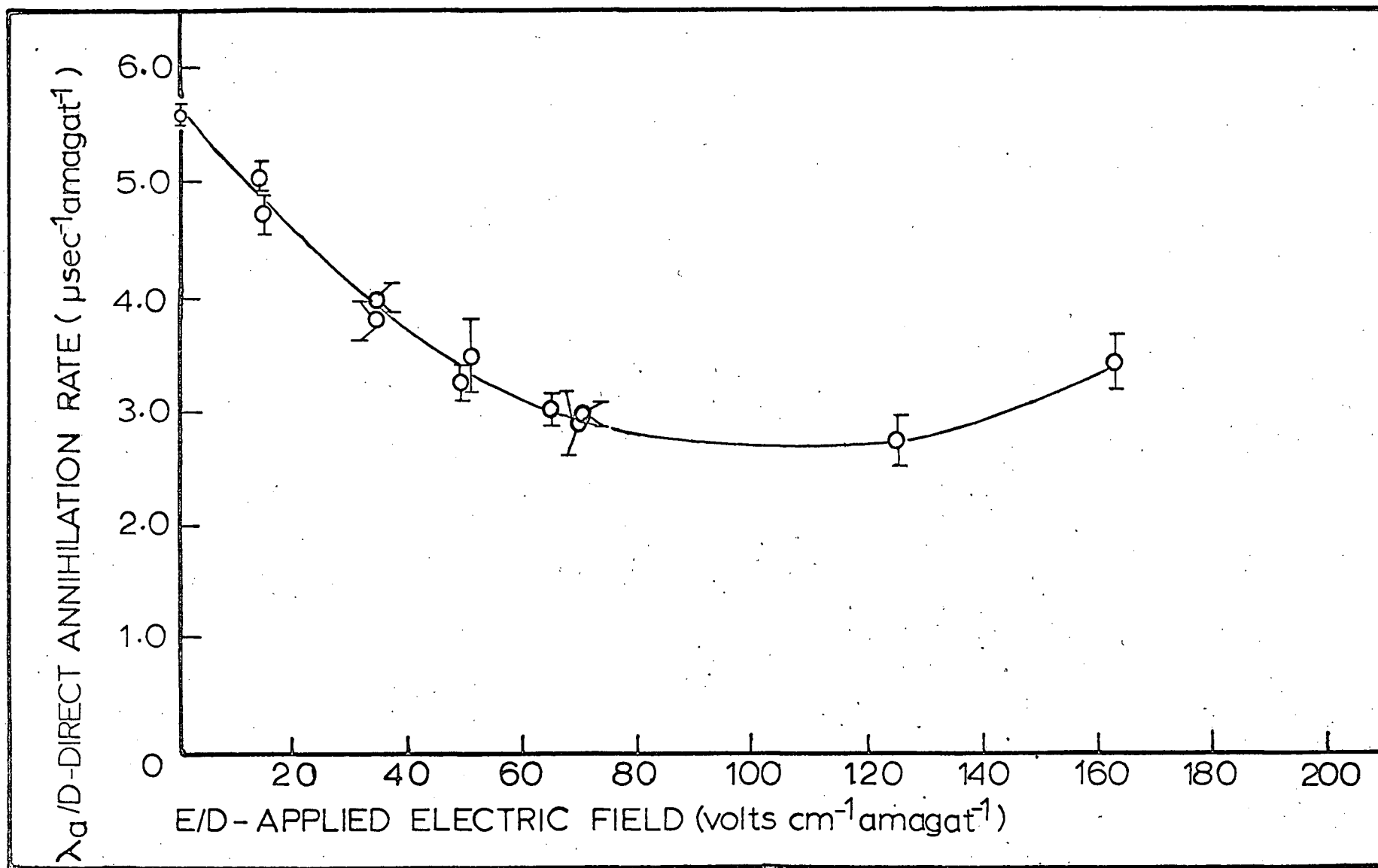


Figure 2: Electric Field Results (Orth, 1966).

the temperature of Argon gas is varied over a limited range. This type of experiment has not been attempted before.

Since raising the temperature of the host gas should have the same effect on the positron velocity as applying an electric field to the gas, and since the shoulder is the slowing down period of positrons in the gas, the shoulder is expected to be shortened if the temperature is raised sufficiently. This would give further information on the velocity dependence of the direct annihilation rate as well as some on the scattering cross-section (Falk et al, 1965).

Orth (1966) found the ortho-positronium annihilation rate in Argon, λ_o , to be

$$\lambda_o = (7.2 \pm 0.4) + (0.29 \pm 0.05)D \times 10^6 \text{ sec}^{-1}.$$

It was also found that the application of an electric field has no effect on the ortho-positronium annihilation rate.

D. Discussion of Velocity Effects on Positron Annihilation in Helium

Falk and Jones (1964) and Falk (1965) report that the direct lifetime in Helium is $0.765 \times 10^6 \text{ sec}^{-1} \text{ am}^{-1}$, and remains constant for densities from 15.2 am to 54.6 am. Falk did not observe any significant shoulder on the time spectra, and the application of an electric field has little effect on the direct lifetime. This indicates that the annihilation rate in Helium is almost velocity independent, in contrast to

the results obtained in Argon.

Present temperature experiments in Helium indicate that the annihilation rate per amagat is essentially constant as a function of temperature. Paul and Graham (1957) report values of $0.78 \times 10^6 \text{ sec}^{-1} \text{ am}^{-1}$ for solid and liquid Helium at 4.2°K . The density of Helium in these cases was 700 am. Roellig and Kelly (1965) report values of $\lambda a/D$ in the range of 0.60 to 0.78 $\text{sec}^{-1} \text{ am}^{-1}$ for gaseous Helium at 4.2°K with densities in the range of 39 to 98 amagats. Hence, it can be seen that for the case of Helium, little or no temperature effect on the direct annihilation rate can be expected. Therefore, at present, there is little evidence for a strong velocity dependence of the direct annihilation rate in Helium.

E. The Justification for Temperature Experiments

As can be seen from the previous arguments, the detailed nature of the dependence of direct positron annihilation rates in noble gases on velocity and hence temperature, is unknown. Therefore, it was thought desirable to build a chamber capable of holding at least 10 amagats of gas over a temperature range from 77°K to 600°K . This would allow an investigation of the effect of temperature on the annihilation rates in various noble gases, especially Argon. Since the temperature

of the gas defines the average velocity of the positrons, the velocity dependence of the annihilation rate can be obtained over a limited range.

The rest of this thesis describes the design of the pressure chamber mentioned above and the experiments carried out using it. The temperature dependence of the direct annihilation rate in Argon, observed between 140°K and 500°K , is reported. The effect of temperature change on the shoulder and the ortho-positronium lifetime is also reported.

CHAPTER II

THE CHAMBER

A. The Design Criteria:

In order to carry out the temperature experiments mentioned in Chapter I, it was necessary to build a chamber that satisfied the following criteria:

1. The vessel must be capable of withstanding pressures of at least 20 atmospheres or 300 psig in the temperature range of 77°K to 600°K. This criterion would allow the use of argon at a density of 10 amagats up to a temperature of 300°C (573°K). It would also allow the use of other gases such as Helium at 20 am. at, and below, room temperature.
2. A provision should be made so that a uniform electric field can be applied to the gas. This required the building of an electric field grid similar to Falk's (1965) and a high voltage feed-through in the chamber lid.
3. The chamber walls must be thin enough so that the gamma rays passing through the walls on the way to the detectors are not attenuated excessively.
4. The chamber's size must be such that not more than 20% to 30% of the positions emitted by a Na²² source in the center of the chamber reach the walls of the chamber with 10 amagats of Argon. This will keep the number of counts in the prompt peak to a

minimum and so allow a more efficient means of counting the direct and ortho-positronium components of the time spectrum.

5. The physical shape and size of the chamber must allow the detectors to be placed about it so as to optimize the counter geometry.

6. The shape and size of the chamber must allow the chamber to be both easily cooled down from room temperature and to be heated above room temperature. The amount of metal in the chamber and the gas volume must be small so that temperature changes can be made quickly and so that the temperature of the gas is uniform about the whole volume employed. In addition, a small chamber is easier to handle when assembling or dismantling.

7. It is also desirable to have a removable lid so that the chamber can be cleaned easily.

B. The Completed Chamber.

Figure 3 shows the chamber finally constructed. It is cylindrical in shape with 1 inch thick plates as lids at either end. The cylinder was turned down around the center so that the wall thickness was $3/16$ inch. There were three holes in the top plate. One was for the gas inlet and outlet, the second was for a thermocouple feed-through, and the third for a high voltage feed-through.

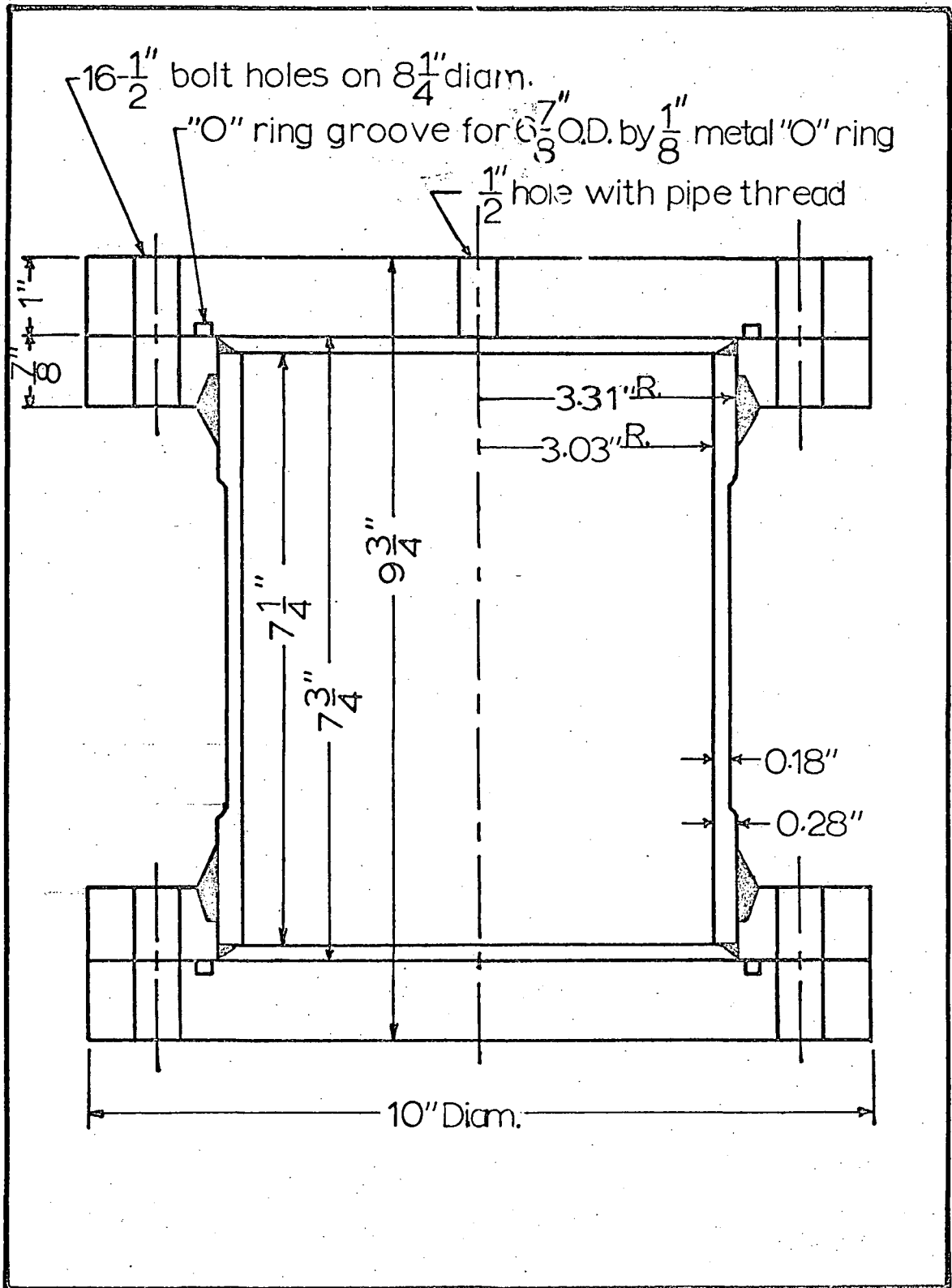


Figure 3: The Chamber.

The way in which this chamber meets the various criteria proposed at the beginning of the chapter will now be considered.

C. The Choice of Material:

Falk (1965) described stainless steel and some aluminum alloys as having the best strength to gamma ray attenuation ratios at room temperatures. Also, the ready availability of these two materials made them very very desirable for use in building a chamber quickly and inexpensively. Since the strength of aluminum at 350°C is degraded much more than the strength of stainless steel at 350°C (see Table 1), 18 - 8 or austenitic stainless steel was chosen as the most suitable material for use in the construction of the chamber.

TABLE I

Ultimate Tensile Strengths at Different Temperatures

| Material | Room Temp | 300 C | 350 C |
|--------------------------------------|-------------------------|-------------------------|-------------------------|
| Al. alloy 2024 Melts at 500-640°C | 70,000 psi ^a | 7,000 psi ^a | 5,000 psi ^a |
| 18-8 stainless steel (annealed) | 75,000 psi ^b | 59,600 psi ^b | 59,400 psi ^b |

a. Alcan (1961).

b. ASME boiler and Pressure Vessel Code (1965).

Note: Alloy 2024 has higher strength than most Aluminum alloys.

Although ordinary carbon steel, like austenitic stainless steel, becomes stronger at low temperatures, it becomes dangerously brittle at these low temperatures (Armstrong, 1959). But, most

important of all, austenitic stainless steel, like copper and aluminum, does not become brittle at low temperatures and it can be used at least to liquid hydrogen temperatures. As an example of the effect of low temperatures on types 304 and 316 stainless steel, Table 2 is included.

TABLE II

Strength and Ductility of Stainless Steel at 298 K and 77 K.

| Type and Temperature | Ultimate Strength (psi) | Elongation before breaking in 2 inches (%) |
|----------------------|-------------------------|--|
| Type 304 S.S. | | |
| 298°K | 90,000 | 65 |
| 77°K | 230,000 | 35 |
| Type 316 S.S. | | |
| 298°K | 84,000 | 70 |
| 77°K | 185,000 | 58 |

(from Superior Catalogue 23, 1965)

It can be seen that the ultimate strength is more than doubled by lowering the temperature to liquid nitrogen temperatures, and that the ductility as indicated by the percentage elongation before breaking is reduced but not enough to make the material dangerously brittle.

Du Mond (1951) lists some of the desirable properties of stainless steels as:

- 1) high corrosion resistance;
- 2) high strength;
- 3) high temperature usability - it has good creep properties;
- 4) it is highly malleable and ductile;

- 5) it can be welded by all of the common processes;
- 6) it can be machined, but strong, high powered tools and special cutting oils are needed; and
- 7) it can be cold or hot worked including being spun.

Some of the undesirable properties of stainless steel are its low thermal conductivity and it is non-hardenable by heat treatment. Stainless steel can be strengthened by cold working but if welding is necessary, the welded metal will be in the neighbourhood of the weld and this will counteract the effects of the cold working.

In view of the above discussion, the materials chosen for the chamber were austenitic stainless steel (types 304 and 316). This choice partially satisfied criteria #1 and #3 stated at the beginning of the chapter.

D. The Shape and Size of the Chamber:

The shape chosen for the chamber was a cylinder with flat plate closings at either end. This shape satisfied criterion #5 for optimally placing counters for the largest count rate and criterion #7 for removable lids. It further satisfies criterion #2 since the cylindrical type of electric field grid, as described by Falk (1965), defines the most constant electric field and allows the use of the largest volume inside the grid. Furthermore, this shape allows one of the flat plate ends of

the chamber to be used for the gas inlet and feed-throughs, while the other end can be used for direct contact with a cold reservoir for low temperature runs. The relatively thin cylindrical walls can be wound with heating tapes to allow the chamber to be heated efficiently. In this way, criterion #6 is fulfilled.

The relatively small size of the chamber satisfied the requirements of criteria #5 and #6 since the small size allowed the counters to be placed close to the source of the gamma rays. Further, the chamber could be heated or cooled with relative ease compared to the large chamber used by Falk (1965) and Orth (1966).

Another advantage of the shape chosen was that the materials for its construction were readily available and were easily assembled since no difficult technique such as metal spinning was involved. In this way the cost of the chamber was held to a minimum.

E. The Number of Positrons Lost in the Walls:

In accordance with criterion #4, the fraction of positrons that annihilate in the walls of the chamber for Argon at 10 amagats will be calculated.

During the experiment the source was set up in the geometrical center of the chamber. The distance to the cylindrical walls of the chamber from the source was then 3 inches or 7.6 cm. For Argon at 10 gm, the range-density product is 76 cm-am.

By referring to Appendix E of Falk (1965), the maximum fraction of positrons reaching the cylindrical walls was found to be 20% of the number emitted in this direction.

The distance from the source to the chamber lids is 3.87 inches or 9.8 cm, making the range-density product equal to 98 cm-am at a gas density of 10 amagats. Therefore, the fraction of positrons emitted in the direction of the lids that reach the lids and annihilate there was calculated to be 8%. It should be noted that when the electric field grid is included in the chamber, this longitudinal distance is reduced to 3 inches.

These considerations indicate that 20% or less of the positrons emitted by the source will annihilate in the walls at a reasonable pressure of 10 atmospheres of Argon at 0°C. This number is not considered too large since Falk and Jones (1964) have reported results at 4.8 am in a spherical chamber with a 14 inch diameter such that 16% of the positrons annihilated in the walls. No adverse events due to wall annihilations were reported. Thus, criterion #4 is satisfied.

F. Gamma-Ray Attenuation:

The cylindrical part of the chamber was turned down on a lathe to a thickness of 0.18 inches in order to decrease the attenuation of gamma rays by the walls. This allows the use

of a thin wall in the region through which the gamma rays must pass while making possible the use of a thick wall at the flange where more strength is needed.

From the Handbook of Chemistry and Physics (1965), the attenuation coefficient, μ/ρ , is $0.080 \text{ cm}^2 \text{ gm}^{-1}$ for gamma rays of 0.50 Mev energy. The density of stainless steel, ρ , is 7.93 gm cm^{-3} and thus μ is 0.635 cm^{-1} . The attenuation of gamma rays is expressed by

$$I/I_0 = \exp (- \mu X) \quad (1)$$

Where I is the intensity of gamma rays before entering the material with attenuation constant μ , and I is the intensity of gamma rays after passing through a distance X of this material.

For 0.18 inches of stainless steel, then, the percentage attenuation as calculated from (1), using $X = 0.18 \text{ in}$, is 25%. Such an attenuation, while substantial, is not excessive. Hence, criterion #3 is fulfilled in total.

G. The Calculation of the Strength of the Chamber.

Since it was anticipated that the chamber would be used at twice room temperature, it was designed to hold at least 10 amagats of Argon at 300°C , that is, it must be capable of holding 300 psi of gas at 300°C .

At 300°C (572°F), the maximum allowable working stress of type 316 stainless steel is 17,100 psi and of type 304 stainless steel is 14,900 psi. These are annealed strengths since it is

suspected that the metal became annealed around the regions in which it was welded. These stresses are those suggested by the ASME code (1965) and allow a safety factor of 4 over the ultimate strength.

1. Cylindrical Walls:

The tangential stress in the cylindrical walls is given by

$$s = \frac{pr}{t}$$

where: p = the allowable pressure in psi;

t = wall thickness = 0.18 in. at the thinnest point;

r = radius of the wall = 3.21 in. average;

and s = maximum stress allowable = 14,900 psi.

Hence, the allowable pressure is 836 psi.

The longitudinal stress is given by $s = \frac{pr}{2t}$ and this gives

an allowable pressure twice that above.

2. Bottom Plate:

The maximum stress in a flat plate with no holes that is freely supported at the edges is given by

$$s = \frac{3(3 + \mu)}{8} p \frac{a^2}{h^2} \quad (\text{Eqn. 99 of Timosheko, 1956}),$$

where: s = maximum allowable stress = 17,100 psi;

μ = Poisson's ratio = 0.33;

p = allowable pressure in psi;

a = radius of plate at bolt circle = 4.125 in; and

$h = \text{effective thickness of plate} = 1.00 \text{ inch.}$

Evaluating this formula gives an allowable pressure of 804 psi.

The maximum stress calculated by this formula occurs at the center of the plate and probably gives an over-estimate of the stress since there is some resisting moment at the edge of the plate, in contrast to the assumption of no resisting moment at the edge of the plate. However, the initial tightening of the bolts will add somewhat to the stresses in the plate. These two effects will probably cancel making the formula a good estimator of the stress in the plate.

3. Top Plate

The top plate has a small hole in the center which means that equation 114 of Timoshenko (1956) has to be used, viz:

$$S = k \frac{pa^2}{h^2}$$

When the particular case that is represented in Figure 4 is used, k is given by Table III from page 114, Timoshenko (1956).

TABLE III

Coefficient k for Equation 114 of Timoshenko (1956)

| <u>a/b</u> | <u>k</u> |
|------------|----------|
| 1.25 | 0.592 |
| 1.5 | 0.976 |
| 2.0 | 1.440 |
| 3.0 | 1.880 |
| 4.0 | 2.080 |
| 5.0 | 2.190 |

With reference to the Table III and the above formula the

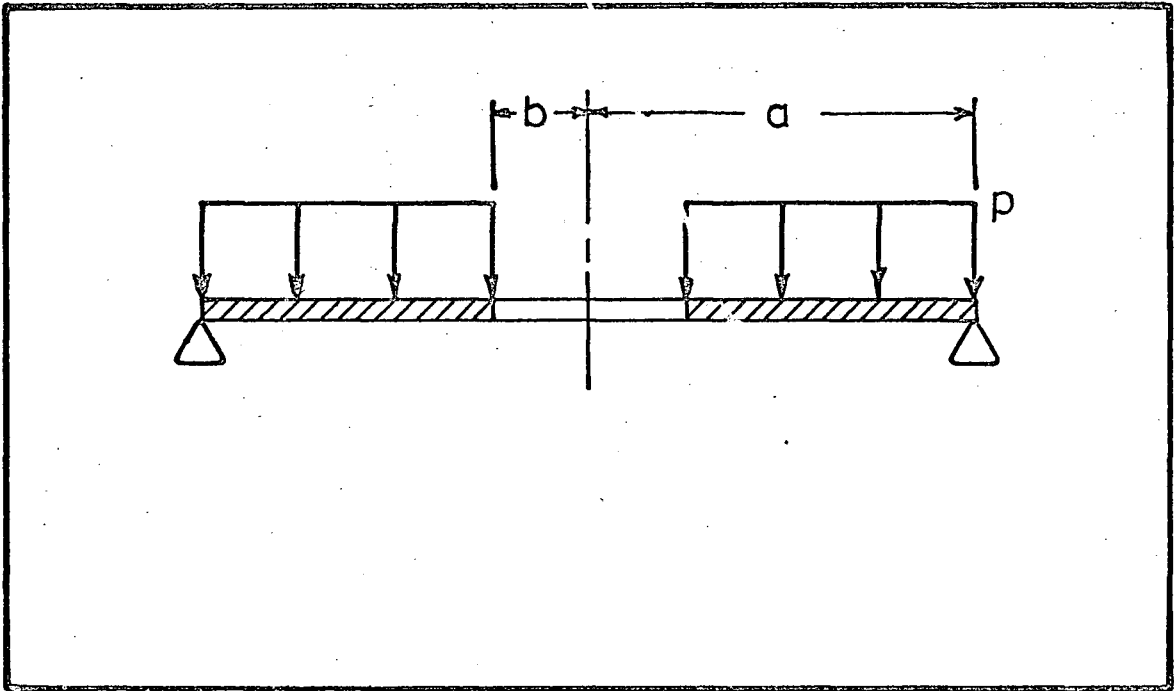


Figure 4: Uniform Load on a Circular Flat Plate with Hole and Freely Supported Edges.

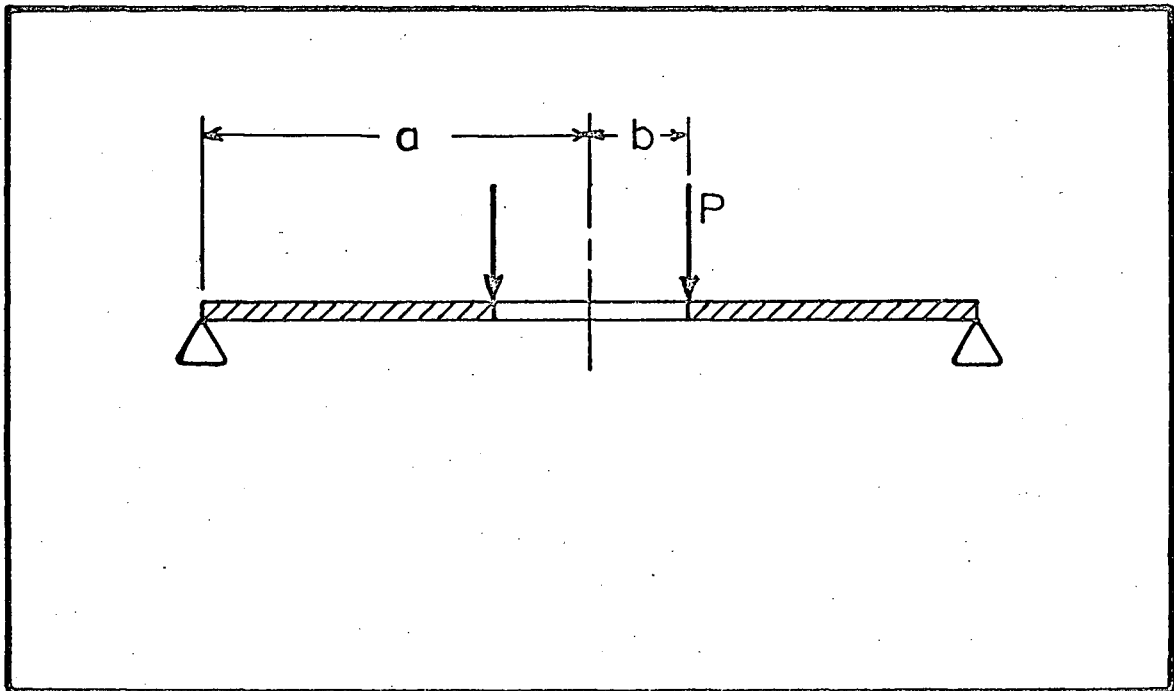


Figure 5: Inner Circle Load on a Circular Flat Plate with Hole and Freely Supported Edges.

the symbols are defined by:

a = radius of the plate = 4.125 in;

b = radius of the hole = 0.25 in;

h = thickness of the plate = 1.00 in;

p = allowable pressure in psi; and

s = maximum allowable stress = 17,100 psi.

For the present case $a/b = 16.5$. By extrapolating Table III to 16.5, k is found to have a value of 2.50. The allowable pressure is then 402 psi.

4. Radial Stress in Flange:

The radial stress in the flange can be estimated by the following formula (see Figure 5):

$$s = \frac{kP}{h^2} \quad (\text{Eqn. 144, Timoshenko, 1956}),$$

where:

s = maximum allowable stress = 14,900 psi;

k = a constant depending upon the ratio b/a ;

P = force per inch acting on the inner edge of the flange =

$$\frac{g^2 p}{2a};$$

h = thickness of flange = 0.9 inch;

b = inner radius of flange = 3.03 inches;

a = bolt circle radius = 4.125 inches; and

g = gasket radius = 3.375 inches.

Since b/a is 1.36 or about 1.5, then k is 1.26 (Case 1, Table 5, Page 114 of Timoshenko, 1956). Therefore, the evaluation of the formula gives an allowable pressure of 6940 psi.

5. Longitudinal Stress in the Flange:

An estimate of the longitudinal stress in the flanges can be obtained by the method used by Falk (1965) in Appendix A. This yields an allowable pressure of 950 psi assuming the maximum safe tensile strength to be 14,900 psi. The complete calculation is shown in Appendix I.

6. Exterior Plumbing:

All fixtures outside of the chamber itself have a pressure rating of at least 4,000 psi. The tubing used to connect the pressure gauge can withstand a pressure of

$$p = \frac{1}{2.3} \frac{t}{r} s = 1300 \text{ psi (Falk, 1965, Appendix A)}$$

at a point where its ends are rigidly fixed. The variables used in the above formula are defined as:

r = radius of the tubing = 0.125 in;

t = thickness of the tubing = 0.025 in; and

s = maximum allowable stress = 14,900 psi.

Throughout these calculations the minimum pressure encountered is 402 psi. This means that the chamber should be able to be used safely at any pressure below this at 300°C.

7. Bolt Load:

The bolt load is given by

$$\text{B.L.} = \pi g^2 p + 2 \pi g I,$$

where g = O-ring radius = 3.375 in;

p = the pressure in the chamber = 300 psi; and

I = the force per inch due to initial tightening =
= 1000 lb/in.

Therefore, the bolt load is 31,900 lb. This means that the bolt load per bolt is 2000 lb, since there are 16 bolts in the top and bottom of the chamber. As the tensile strength of a 1/2 inch stainless steel bolt is 2,260 psi (Superior Tube catalogue, 1965), the bolt strength is adequate.

H. The Pressure Test of the Chamber:

The chamber was pressure tested by filling it with water and applying pressure to the water using a tube connected to a bottle of compressed air. The pressure was cycled up to 800 psi three times, being increased in quick steps of about 60 psi into the 700-800 psi range.

No signs of distortion or leaks were detected during this test. It was concluded that the chamber was quite safe to use for pressures of at least 400 psi by allowing a safety factor of 2 over the tested pressure. Since the chamber was tested at room temperatures, allowance must be made for the decrease in strength at 300°C. The safe operating pressure is given by

$$P_{300} = P_0 \frac{S_{300}}{S_0}$$

Since $S_{300} = 14900$ psi and $S_o = 18750$ psi, the safe operating pressure at 300°C is 318 psi.

The chamber is, therefore, capable of holding 300 psi of gas at 300°C , thus completely fulfilling the first requirement for the chamber.

I. The Electric Field Grid:

An electric field grid was constructed with a design similar to that of Falk (1965). The grid that was constructed for this chamber was made 6 inches long by $5\frac{1}{2}$ inches in diameter. Rings of $\frac{1}{8}$ inch diameter were spaced at intervals of $\frac{1}{2}$ inch, with flat plates at either end of the grid. The center grid was made so that wires could be strung on it so as to hold the Na^{22} source. The rings were connected by 22 Megohm resistors, which acted as a voltage dividing network and so defined the electric field.

In order to achieve an electric field of 1.22 Kv-cm^{-1} as did Falk (1965), a potential of 11 Kilovolts must be applied to the end plates of the electric field grid. Since the top plate of the grid was 0.64 cm from the wall of the chamber, an electric field of 17.3 Kv-cm^{-1} will be formed between the chamber wall and the top plate. The electric breakdown voltage of Argon is 80 Kv-cm^{-1} at 10 am. Hence, at least 11 Kv should be able to remain on the end plates of the grid without breakdown occurring.

CHAPTER IIIEXPERIMENTAL DETAILSA. Experimental Set-up of Electronics

The electronics used to collect the data for the time spectra were set up in almost the same configuration as that used by Orth (1966). There were however two major differences. First, the energy pulse was taken from the last dynode, along with the timing pulse, rather than from an intermediate dynode as was done previously. Second, the 256 channel kick-sorter was replaced by a 400 channel, PIP 400 Victoreen kick-sorter with a paper tape readout. A block diagram of the electronics used is shown in Figure 6.

Both the differential and integral linearities of the timesorter were measured before the experiments started. A graph showing the integral linearity is displayed in Figure 7. The integral linearity check showed that the time per channel was 1.57 nsec. The time per channel figure was checked during the runs by inserting a 244 nsec delay cable into the 0.51 Mev (delayed) line and noting the number of channels through which the prompt peak shifted. The result confirmed the figure of 1.57 nsec/channel which was being used. The differential linearity check (Figure 8) in which an average of 6600 counts were obtained in each channel, indicated that the time sorter was linear except for the top

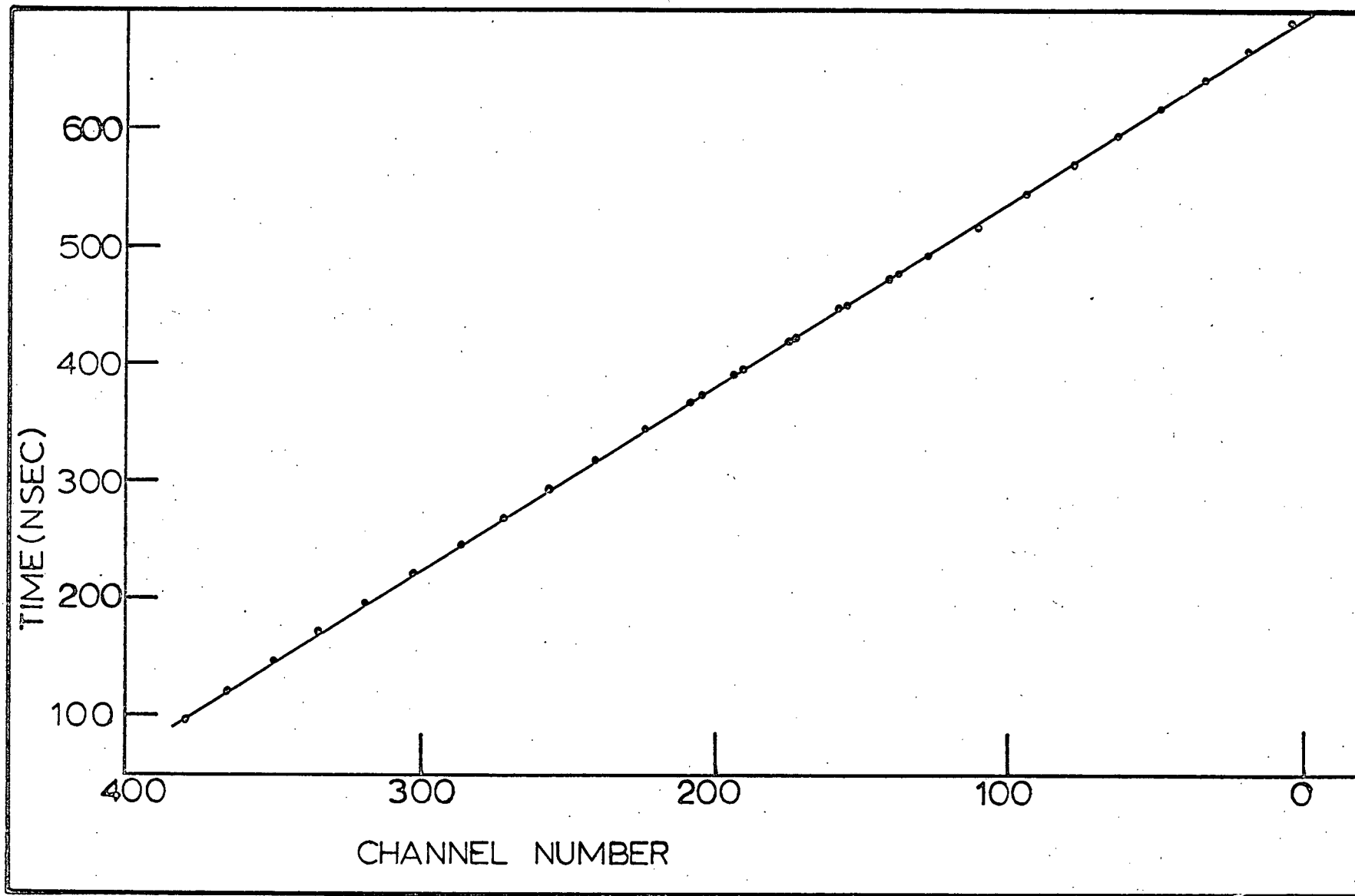


Figure 7: Integral Linearity of the Time Sorter.

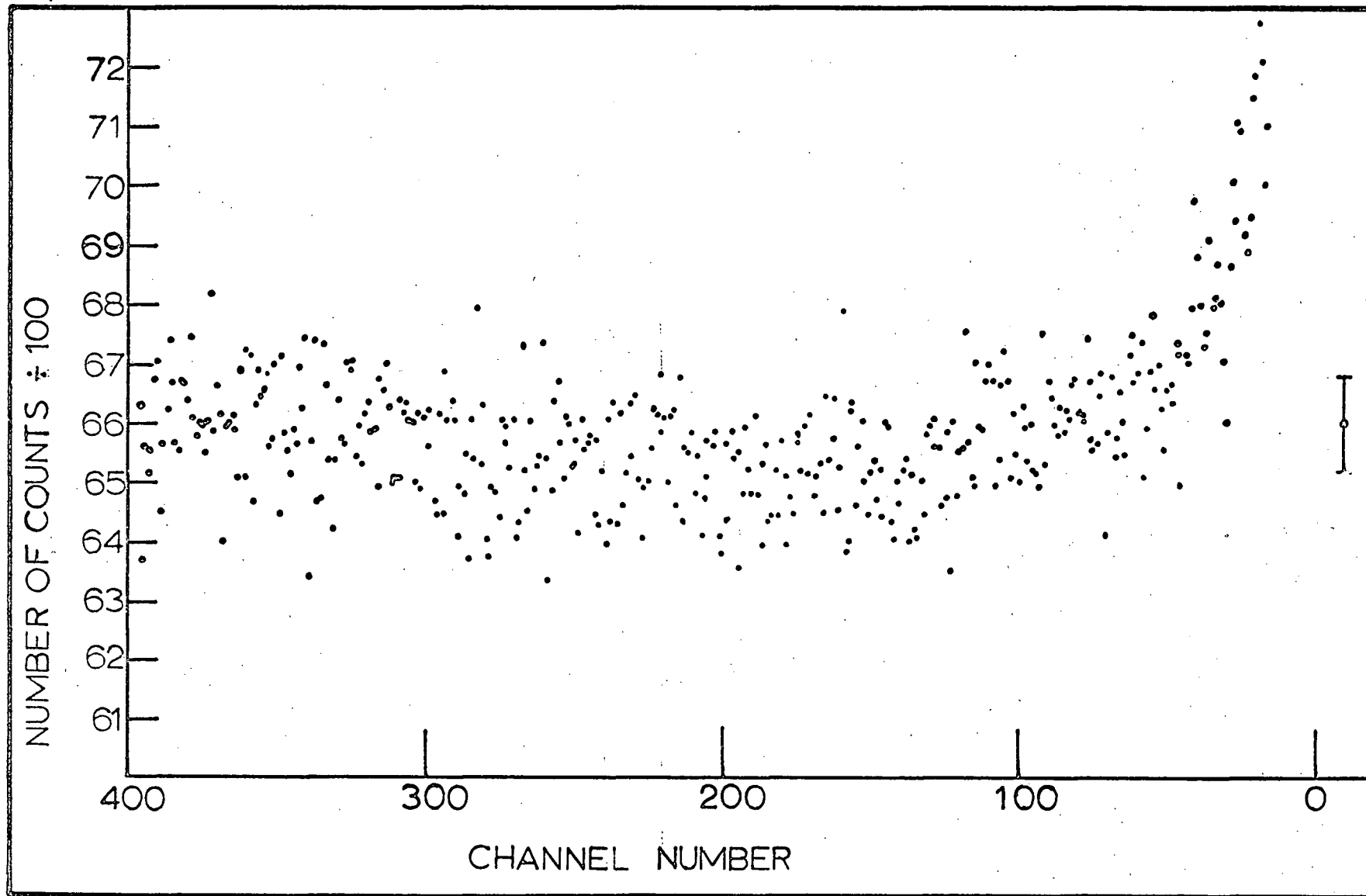


Figure 8: Differential Linearity of the Time Sorter.

40 channels. The data from the two linearity measurements were used in the analysis of the results obtained from the time sorter.

The time resolution of the system varied from 4.5 to 5.5 channels (7.1 to 8.6 nsec) full width half maximum on the prompt peak. The time resolution of the system was measured with a Na^{22} source in Aluminum: once, before the experiments were started and again almost at the completion of the experiments. The first result gave a time resolution of 4.6 channels (7.2 nsec) and the second result gave a time resolution of 4.8 channels (7.6 nsec). This variation in resolution was caused by the varying counter geometries, count rates, and single channel analyser window settings during the course of the experiment.

B. The Preparation of the Chamber for Temperature

Variation:

To measure the temperature of the gas inside the chamber a thermocouple lead-through was fitted into the top plate of the chamber. One of the junctions of a chromel-alumel thermocouple was placed inside the chamber immersed in the gas itself. The other junction was placed either in an ice bath or in the air at room temperature. The voltage across the thermocouple was measured by a Hewlett-Packard 410 C V.T.V.M. On this instrument the voltage could be estimated to 0.02 millivolts (about 0.5°C). The input resistance of the V.T.V.M. was 1.00 Megohm and the claimed accuracy over

the range on which it was being used is 2%. A measurement made of the difference between room temperature, 298°K, and liquid nitrogen temperature, 77°K, showed the device to be in error by less than 1%.

Since runs were done for both temperatures above and below room temperature the description of the experimental preparation of the chamber will be divided into the high temperature set-up (above room temperature) and the low temperature set-up (below room temperature).

1) The High Temperature Set-up:

In order to heat the chamber above room temperature the walls of the chamber were electrically heated. This was done by placing a thin sheet of mica around the thin cylindrical chamber walls and then winding a heating element consisting of 20 guage nichrome wire over the mica. The whole assembly was covered with a layer of asbestos cloth which in turn was covered with a layer of shiny aluminum foil. The temperature of the chamber was controlled by varying the current through the element using a variac. The highest temperature obtained during the experiment was 232°C during the bake out of the chamber.

2) The Low Temperature Set-up:

To obtain temperatures below ambient the chamber was turned upside down and placed in a styrefoam container, as shown in Figure 9. A cylindrical metal container was placed on the bottom flat plate of the chamber, inside the syrefoam

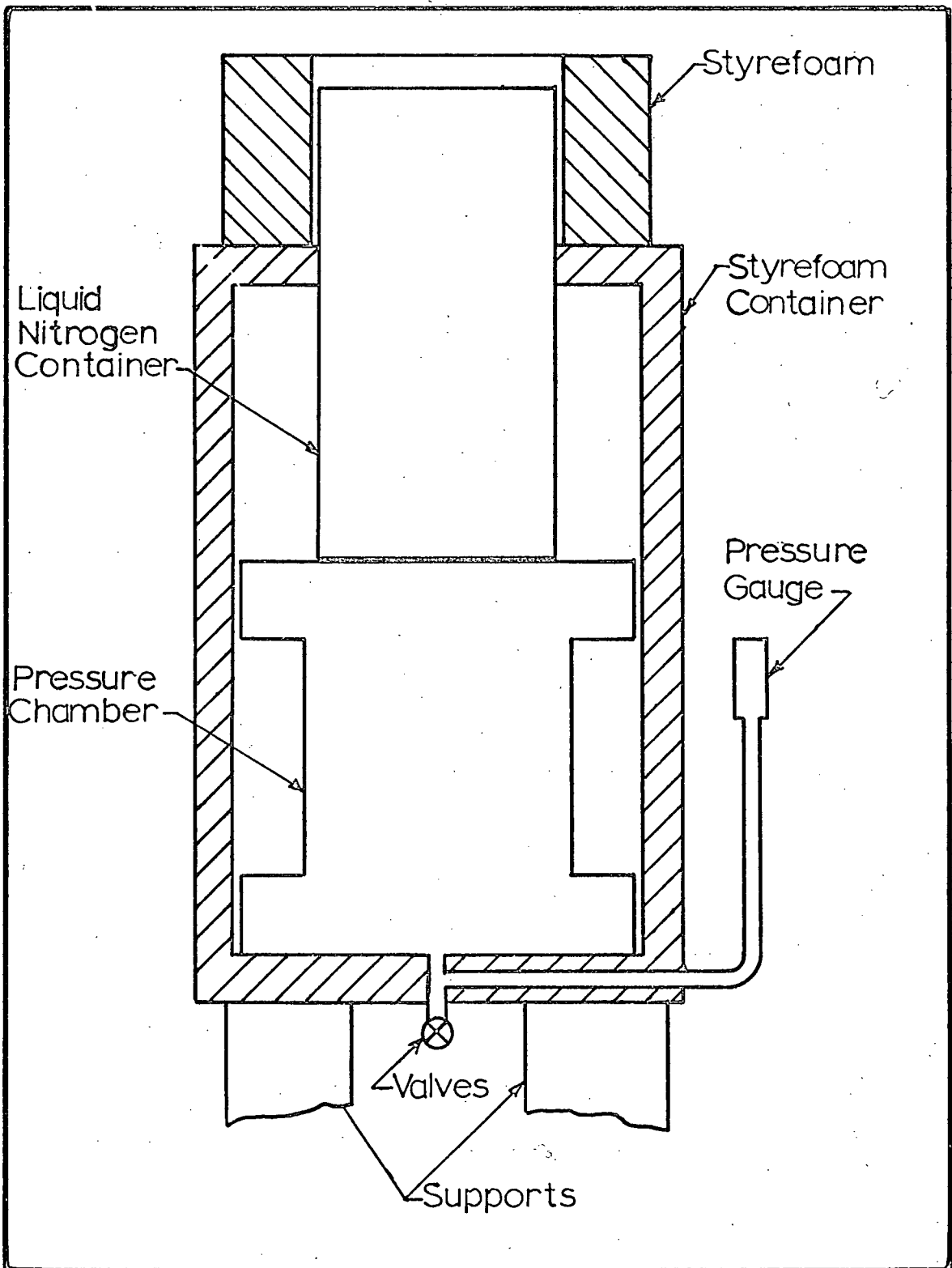


Figure 9: The Low Temperature Configuration.

box. This container was then filled with liquid nitrogen thus cooling the chamber and the gas. The lowest recorded temperature during the experiment was 1.10° K.

C. The Gas Filling:

High gas purities are necessary to obtain good experimental results. The results of Tao and Bell (1967) on minor impurities in Argon show that a small percentage of impurities can have a large influence on these results. These results indicate that the shoulder is very sensitive to some impurities.

In order to obtain as high a gas purity as possible inside the chamber, Argon with a purity of 99.999% was purchased from Matheson of Canada, Ltd. Before filling the chamber with the gas it was evacuated to 10^{-4} - 10^{-3} torr with a vacuum pump. Then it was heated under vacuum to a temperature at least 25° C above that at which the experiment was to take place in order to degas the chamber walls as much as possible. The chamber was then flushed at least three times to a pressure of not less than 3 atmospheres with the gas it was to be filled with. The chamber was then allowed to cool to room temperature under vacuum and then it was flushed three more times to 3 or more atmospheres with the gas before it was filled to the desired pressure.

Finally, a check of gas purity was made by monitoring the width of the shoulder with time. As has been mentioned above, the shoulder width is very sensitive to gas impurities.

The effectiveness of this purity check was tested during the experiment by heating the chamber to a temperature above that at which the chamber was outgassed. The result was that the shoulder width decreased from 350 nsec-am to 230 nsec - am and the direct annihilation rate was increased from 5.4 $\mu\text{sec}^{-1} \text{ am}^{-1}$ to 6.7 $\mu\text{sec}^{-1} \text{ am}^{-1}$. No change was noticed in the ortho-positronium lifetime.

CHAPTER IV

PRESENTATION OF RESULTS

A. The Scope of the Results:

The temperature results were collected in Argon at two different densities, 8.0 and 10.2 amagats. For the 8.0 amagat results the temperature was varied between 143°K and 450°K while for the 10.2 amagat runs the temperature was varied between 144°K and 480°K. In all the recorded spectra the temperature was controlled to within $\pm 3^\circ$ of the average value.

B. The Analysis of the Time Spectra:

Each time spectrum was fitted to the analytic form

$$N = I_1 \exp(-t/t_1) + I_2 \exp(-t/t_2) + B,$$

where: N = the number of counts at time t ;

I_1 = the intensity of the direct component;

t_1 = the lifetime of the direct component;

I_2 = the intensity of the ortho-positronium component;

t_2 = the lifetime of the ortho-positronium component;

and B = the intensity of the random background.

The analysis of the time spectra was undertaken by the maximum likelihood method using a computer program developed by Orth (1966). The program incremented all five parameters to obtain the best fit. The spectra were fitted using the data in the negative time region behind the prompt peak and

between the shoulder and channel number 380 in the positive time region. The differential linearity results (see Chapter 3) were used to define relative channel widths and the integral linearity result was used to change number of channels into time.

C. The Results:

The results of the maximum likelihood fits are displayed in table IV. Shown in this table is the run number, the direct lifetime (τ_a), the ortho-positronium lifetime (τ_o), the direct annihilation rate (λ_a), the ortho-positronium annihilation rate (λ_o), the density (D), the temperature (T), the ratio λ_a/D , the shoulder width-pressure product (SD), and the probability of obtaining a worse fit (Q). Essentially two sets of results are shown in Table IV: those at 8.0 amagats with varying temperatures and those at 10.2 amagats with varying temperatures.

For a time spectrum to be accepted it was necessary that the spectrum satisfy the following criteria:

1. The maximum likelihood fit was started at least five channels beyond the shoulder's edge.
2. The chi-square of the final fit was the lowest of all fits made on that particular spectrum satisfying criterion 1. In the case of two almost equivalent chi-squares the spectrum fit closest to the shoulder (with the most points) was accepted. All fits ended in channel 380.

TABLE IV

Results From the Maximum Likelihood Fit

| RUN | τ_a (nsec) | τ_o (nsec) | λ_a (μsec^{-1}) | λ_o (μsec^{-1}) | D (am) | T ($^{\circ}\text{K}$) | λ_a/D ($\mu\text{sec}^{-1}\text{am}^{-1}$) | S.D (ns-am) | Q |
|-----|--------------------|--------------------|---|---|-----------|-----------------------------|---|----------------|-----|
| T1 | 18.6-0.6 | 90.0-3.2 | 53.8-1.7 | 11.1-0.4 | 9.89 | 298 | 5.44-0.18 | 349 | .02 |
| T6 | 17.6-0.6 | 96.2-7.3 | 56.8-1.9 | 10.4-0.8 | 10.56 | 299 | 5.38-0.18 | 332 | .42 |
| T15 | 18.6-0.6 | 92.7-5.3 | 53.8-1.7 | 10.8-0.6 | 8.03 | 143 | 6.70-0.22 | 336 | .04 |
| T17 | 21.9-0.7 | 94.9-6.3 | 45.7-1.5 | 10.5-0.7 | 8.03 | 215 | 5.69-0.18 | 366 | .46 |
| T18 | 20.3-0.9 | 87.1-5.9 | 49.3-2.2 | 11.5-0.8 | 8.03 | 175 | 6.13-0.27 | 366 | .79 |
| T19 | 22.3-1.0 | 94.0-7.1 | 44.8-2.0 | 10.6-0.8 | 8.03 | 260 | 5.58-0.25 | 366 | .79 |
| T20 | 21.8-0.8 | 93.2-4.5 | 45.9-1.7 | 10.7-0.5 | 8.03 | 295 | 5.71-0.21 | 353 | .10 |
| T21 | 25.1-0.8 | 104.9-5.8 | 39.8-1.3 | 9.5-0.5 | 8.03 | 296 | 4.96-0.16 | 353 | .73 |
| T22 | 24.8-0.9 | 91.9-5.1 | 40.3-1.5 | 10.9-0.6 | 8.03 | 390 | 5.02-0.18 | 366 | .04 |
| T23 | 25.9-0.8 | 94.6-4.8 | 38.6-1.2 | 10.6-0.5 | 8.03 | 449 | 4.81-0.15 | 341 | .93 |
| T26 | 18.0-0.5 | 89.7-4.1 | 55.6-1.5 | 11.1-0.5 | 10.22 | 299 | 5.44-0.15 | 337 | .01 |
| T27 | 14.5-0.4 | 93.0-3.9 | 69.0-1.9 | 10.8-0.5 | 10.22 | 144 | 6.75-0.19 | 337 | .18 |
| T28 | 16.3-0.5 | 90.1-4.3 | 61.3-1.9 | 11.1-0.5 | 10.22 | 215 | 6.00-0.18 | 353 | .50 |

cont...TABLE IV

| RUN | τ_a (nsec) | τ_o (nsec) | λ_a (μsec^{-1}) | λ_o (μsec^{-1}) | D (am) | T ($^{\circ}\text{K}$) | λ_a/D ($\mu\text{sec am}^{-1}$) | S.D. (ns-am) | Q |
|-----|--------------------|--------------------|---|---|----------------------|-----------------------------|--|-----------------|-----|
| T29 | 16.1 \pm 0.6 | 88.9 \pm 4.5 | 62.1 \pm 2.3 | 11.2 \pm 0.6 | 10.22 | 192 | 6.08 \pm 0.23 | 353 | .50 |
| T30 | 17.1 \pm 0.7 | 90.8 \pm 4.7 | 58.5 \pm 2.4 | 11.0 \pm 0.6 | 10.22 | 236 | 5.72 \pm 0.23 | 353 | .54 |
| T31 | 17.8 \pm 0.5 | 86.7 \pm 3.8 | 56.2 \pm 1.6 | 11.5 \pm 0.5 | 10.22 | 297 | 5.50 \pm 0.15 | 372 | .76 |
| T32 | 18.5 \pm 0.7 | 86.9 \pm 4.8 | 54.1 \pm 2.0 | 11.5 \pm 0.6 | 10.22 | 343 | 5.29 \pm 0.20 | 338 | .42 |
| T33 | 19.6 \pm 0.8 | 87.6 \pm 5.3 | 51.0 \pm 2.1 | 11.4 \pm 0.7 | 10.22 | 393 | 4.99 \pm 0.20 | 369 | .73 |
| T35 | 21.9 \pm 0.7 | 100.0 \pm 7.3 | 45.7 \pm 1.5 | 10.0 \pm 0.7 | 10.22 | 444 | 4.47 \pm 0.14 | 353 | .96 |
| T36 | 19.1 \pm 0.6 | 83.2 \pm 4.2 | 52.4 \pm 1.6 | 12.0 \pm 1.6 | 10.22 | 445 | 5.12 \pm 0.16 | 370 | .34 |
| T37 | 20.3 \pm 1.1 | 89.5 \pm 5.9 | 49.3 \pm 2.7 | 11.2 \pm 0.7 | 10.22 | 480 | 4.82 \pm 0.26 | 369 | .07 |
| T38 | 18.2 \pm 0.5 | 90.9 \pm 3.8 | 54.9 \pm 1.5 | 11.0 \pm 1.5 | 10.22 | 296 | 5.38 \pm 0.15 | 338 | .69 |
| T39 | 18.1 \pm 0.6 | 91.2 \pm 4.2 | 55.2 \pm 1.8 | 11.0 \pm 0.5 | 10.22 | 295 | 5.41 \pm 0.18 | 354 | .73 |
| T40 | 20.5 \pm 0.5 | 96.1 \pm 4.3 | 48.8 \pm 1.2 | 10.4 \pm 0.5 | 9.47 | 295 | 5.15 \pm 0.13 | 369 | .82 |

3. The number of counts in the shoulder was at least 1000.
4. The electronics remained stable during the run, that is, the prompt peak remained stationary during the run,
5. The shoulder width-density product remained constant to within 10%.
6. The chi-square gave a probability of obtaining a worse fit of 1% or better.
7. The temperature did not vary more than 5°K during the run.
8. Finally, the maximum likelihood program converged on all 5 parameters for each of these runs.

It should be noted here that the ortho-positronium lifetime was not as well defined in these results as it was in those of Orth (1966). Since the source strength used in this experiment was greater than that used by Orth, the true to chance count ratio was decreased. In this way the random background was increased at the expense of the ortho-positronium component. In addition, a rather narrow window width about the 0.51 Mev peak was used in order to enhance the collection of two photon events, again at the expense of three photon or ortho-positronium events.

D. The Interpretation of the Results:

1) The Temperature Dependence of the Direct Annihilation Rate. λ_a :

Figure 10 shows a graph of the direct annihilation rate per amagat, λ_a/D , plotted against temperature, T. The main feature of the curve is that the annihilation rate decreases

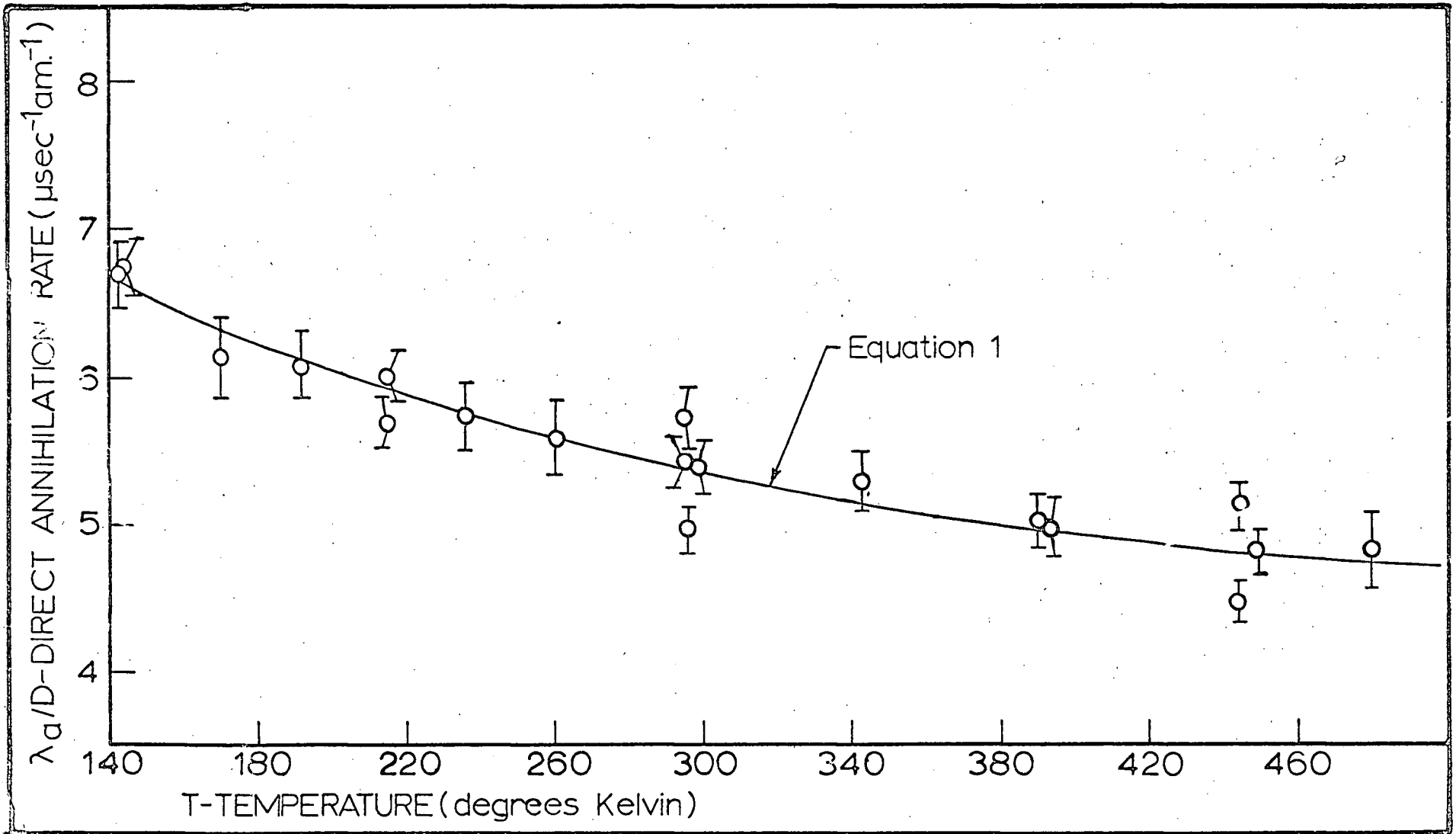


Figure 10: A Graph of the Direct Annihilation Rate per Amagat, λ_a/D , Plotted against Temperature, T .

as temperature increases. This indicates that the direct annihilation rate is a decreasing function of velocity over the range investigated. The above dependence on velocity agrees in its general form with the electric field results for Argon first reported by Falk et al (1965).

The average thermal velocity of the positron, V_0 , depends on the temperature of the gas, T , in such a way that V_0 is proportional \sqrt{T} . Therefore, least squares fits to the results were made using polynomials in \sqrt{T} and T , in anticipation of expressing the annihilation rate as polynomials in v and v^2 (see section E of this chapter), where v is the velocity of the positron. These polynomials were fitted so as to give a finite annihilation rate at zero velocity. This step was taken since the Dirac equation predicts a constant annihilation rate at small velocities (see ~~Orth and Jones~~, ^{Jones and Orth}, 1967). A logarithmic form of the annihilation rate was also fitted to the results in order to compare the result with that of Jones et al (1965).

Examination of the results in Table V shows that, of those fits that have a finite intercept at $T=0$, the best fit is;

$$\frac{\lambda_a(T)}{D} = 11.9 \pm 1.3 - 5.73 \pm 1.58 \times 10^{-1} \sqrt{T} + 1.12 \pm .46 \times 10^{-2} T$$

$$\mu\text{sec}^{-1} \text{am}^{-1} \quad (1)$$

since it has the highest Q value of these fits. It is emphasized that all of the fits (Table V) to the experimental data are only correct for the temperature range investigated,

TABLE V

Results of Fitting $\lambda a / D$ versus T by Least Squares

| POLYNOMIAL FITTED. | CONSTANTS | | | | Q |
|-----------------------|----------------------------|--|----------------------------------|------------------------------------|-----|
| | A ($\mu s^{-1} am^{-1}$) | B ($\mu s^{-1} am^{-1}$) | C ($\mu s^{-1} am^{-1}$) | D ($\mu s^{-1} am^{-1}$) | |
| F (\sqrt{T}) | | $\times 10^{-1} \text{deg}^{-\frac{1}{2}}$ | $\times 10^{-2} \text{deg}^{-1}$ | $\times 10^{-3} \text{deg}^{-3/2}$ | |
| Order 1 | $8.68 \pm .25$ | $-1.88 \pm .14$ | | | .11 |
| Order 2 | 11.9 ± 1.3 | -5.73 ± 1.58 | $1.12 \pm .46$ | | .29 |
| Order 3 | 21.5 ± 10.1 | -23.5 ± 18.7 | 11.9 ± 11.3 | -2.13 ± 2.24 | .19 |
| F(T) | | $\times 10^{-2} \text{deg}^{-1}$ | $\times 10^{-5} \text{deg}^{-2}$ | $\times 10^{-8} \text{deg}^{-3}$ | |
| Order 1 | $7.07 \pm .13$ | $-.534 \pm .041$ | | | .02 |
| Order 2 | $8.39 \pm .40$ | $-1.45 \pm .26$ | $1.44 \pm .41$ | | .25 |
| Order 3 | 9.93 ± 1.36 | -3.24 ± 1.53 | 7.81 ± 5.37 | -7.00 ± 5.89 | .26 |
| F(lnT) | | | | | |
| Order 1 | $3.31 \pm .12^*$ | $-0.285 \pm .021$ | | | .40 |

*Note: $\exp(3.31 \pm .12) = 27.4 \pm 3.3$

that is, 143° K to 480° K. This fit (equation 1) to the results goes through a minimum at 654° K with $\lambda_a/D = 4.6 \mu\text{sec}^{-1} \text{am}^{-1}$, whereas previous results with an electric field (Orth, 1966) indicate that the minimum value of λ_0/D is at least as small as $2.6 \mu\text{sec}^{-1} \text{am}^{-1}$. Therefore, equation 1 above is not considered to give a good estimate of the direct annihilation rate above 480° K.

The logarithmic fit

$$\frac{\lambda_a(T)}{D} = \frac{27.4 \pm 3.3}{T} \mu\text{sec}^{-1} \text{am}^{-1} \quad (2)$$

$$\frac{-0.285 \pm 0.021}{T}$$

is expected to give a better interpolated value of the annihilation rate at temperatures higher than 480° K because it is a continuously decreasing function of temperature, T. Unfortunately, equation 2 does not tend to a finite value as $T \rightarrow 0^\circ \text{K}$, and so gives poor values at very low temperatures.

2) The Temperature Dependence of the Orthopositronium

Annihilation Rate, λ_0 :

Figure 11 shows a graph of λ_0 plotted against T for 8.0 amagats and 10.2 amagats. Table VI shows the results of fitting the experimental points to polynomials in T using the least squares method. The results presented here indicate that there is no large temperature effect on the ortho-positronium lifetime in Argon. The average annihilation rates are $11.1 \pm 0.2 \mu\text{sec}^{-1}$ at 10.2 am and $10.5 \pm 0.2 \mu\text{sec}^{-1}$ at 8.0 am.

3) The Dependence of the Direct Rate on Density:

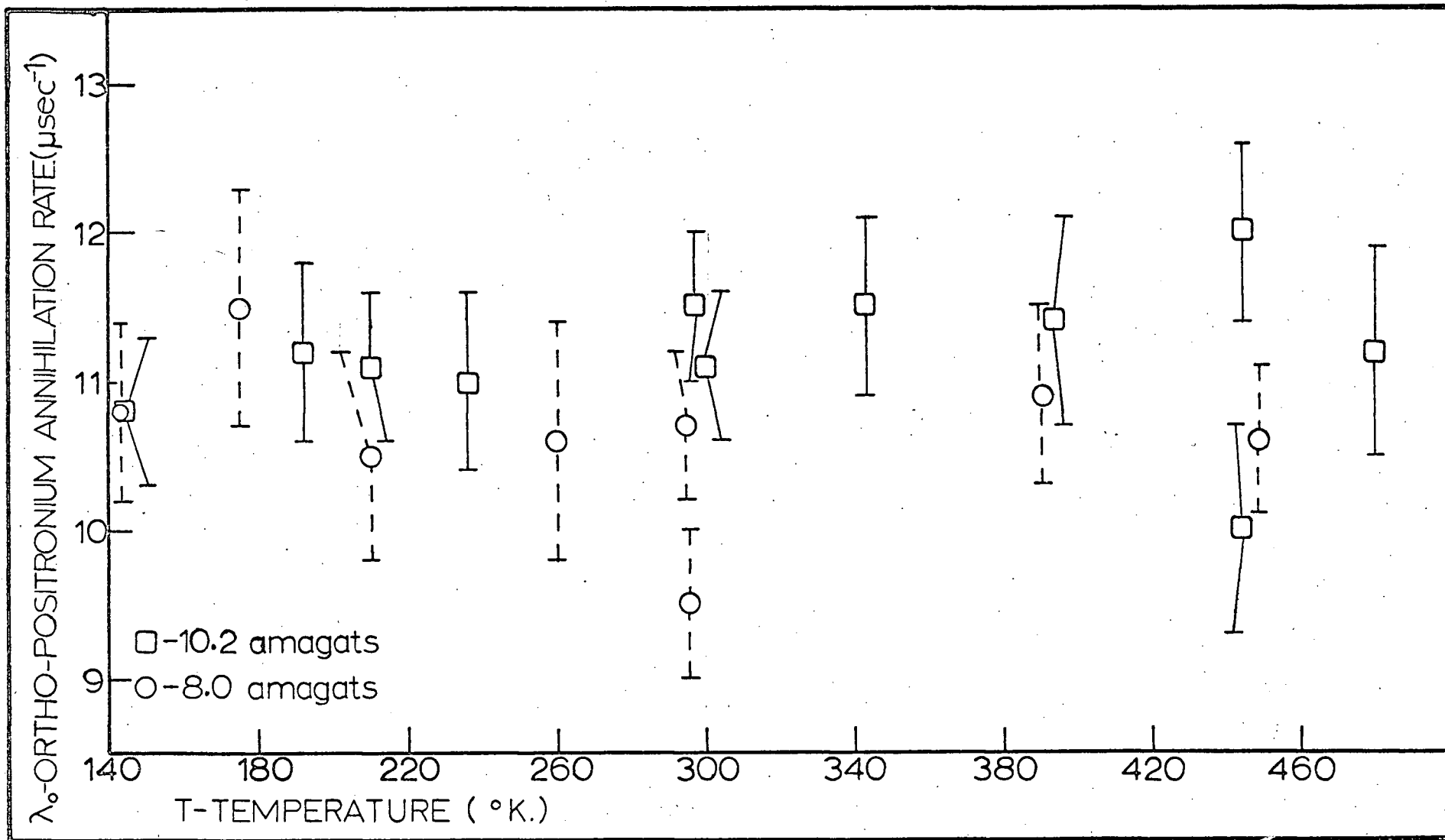


Figure 11: A Graph of the Ortho-Positronium Annihilation Rate, λ_o , Plotted against Temperature, T.

TABLE VI

Results of Fitting λ_0 versus T by Least Squares

| <u>COMMENTS</u> | <u>CONSTANTS</u> | | <u>Q</u> |
|--------------------|-------------------------------|--|----------|
| | A (μsec^{-1}) | B ($\mu\text{sec}^{-1}\text{deg}^{-1}$) | |
| 8.0 AM. Fits | | | |
| Order 1 Polynomial | $10.75 \pm .67$ | $-7.16 \pm 21.25 \times 10^{-4}$ | .40 |
| Order 0 Polynomial | $10.54 \pm .21$ | | .49 |
| 10.2 AM. Fits | | | |
| Order 1 Polynomial | $10.85 \pm .52$ | $1.00 \pm 1.67 \times 10^{-3}$ | .87 |
| Order 0 Polynomial | $11.14 \pm .16$ | | .89 |

Figure 12 shows the direct annihilation rate, λ_a , plotted against density, D , at 297°K. Table VII shows the results of fitting various polynomials in D to these results. It is evident that these results indicate a value of $\lambda_a/D = 5.4 \pm 0.1 \mu\text{sec}^{-1}\text{am}^{-1}$ between 8 and 11 amagats. This result agrees with that of Orth (1966) at $5.6 \pm 0.1 \mu\text{sec}^{-1}\text{am}^{-1}$ (that is, the present results are within two standard deviations of Orth's result). This agreement at 297°K is necessary in order to compare these temperature results with those for an applied electric field (Orth, 1966), as will be done in part F of this chapter.

4) The Density Dependence of the Ortho-positronium Annihilation Rate:

Figure 13 shows the dependence of λ_0 on D at room temperature. It is obvious that there is considerable scatter in these results. The results of fitting the orthopositronium points by least squares are shown in Table VIII. Both room temperature results and all results taken regardless of temperature were fitted. For an assumed vacuum annihilation rate of $7.2 \mu\text{sec}^{-1}$ the quenching rate is $0.39 \mu\text{sec}^{-1}\text{am}^{-1}$ if all the results are used. The best estimate of a standard deviation for this result is considered to be the standard deviation calculated for λ_q , the quenching rate, by the least squares fit to $\bar{\lambda}_0 + \lambda_q D$. Then, the standard deviation of λ_q is $0.12 \mu\text{sec}^{-1}\text{am}^{-1}$.

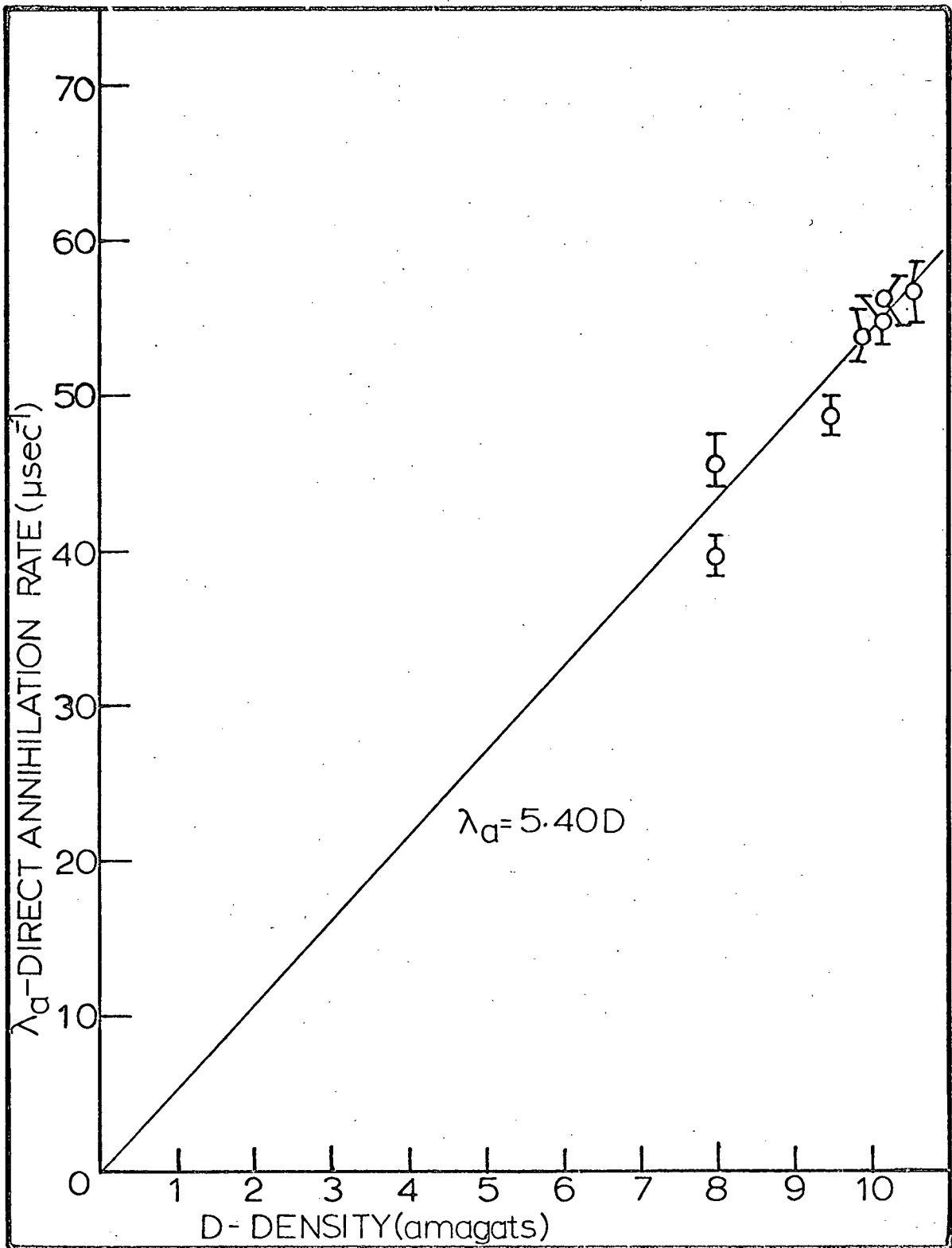


Figure 12: A Graph of the Direct Annihilation Rate, λ_a , Plotted against Density, D .

TABLE VII

Results of Fitting λ_D versus D by Least Squares

| <u>COMMENTS</u> | <u>CONSTANTS</u> | | | Ω |
|---------------------------------|-------------------------------|---|---|----------|
| | A (μsec^{-1}) | B ($\mu\text{sec}^{-1}\text{am}^{-1}$) | C ($\mu\text{sec}^{-1}\text{am}^{-2}$) | |
| 8.- 11. am. fits | | | | |
| Order 1 Polynomial | 0 | $5.37 \pm .06$ | | .20 |
| Order 1 Polynomial | -6.30 ± 5.45 | $6.03 \pm .57$ | | .20 |
| $\lambda_D/D = \text{Constant}$ | 0 | $5.40 \pm .07$ | | .58 |
| Order 2 Polynomial | 0 | $4.50 \pm .64$ | $0.086 \pm .066$ | .16 |

TABLE VIII

Results of Fitting λ_0 versus D by Least Squares

| <u>COMMENTS</u> | <u>CONSTANTS</u> | | Ω |
|--|-------------------------------|---|----------|
| | A (μsec^{-1}) | B ($\mu\text{sec}^{-1}\text{am}^{-1}$) | |
| Fits to Room Temperature Results | | | |
| Order 1 Polynomial | 6.52 ± 1.83 | $.45 \pm .19$ | .65 |
| $\bar{\lambda}_0 = 7.2$, Order 1 | 0 | $.37 \pm .02$ | .64 |
| Fits to All Results Independent of Temperature | | | |
| Order 1 Polynomial | 8.47 ± 1.12 | $0.26 \pm .12$ | .87 |
| $\bar{\lambda}_0 = 7.2$, Order 1 | 0 | $0.39 \pm .01$ | .85 |

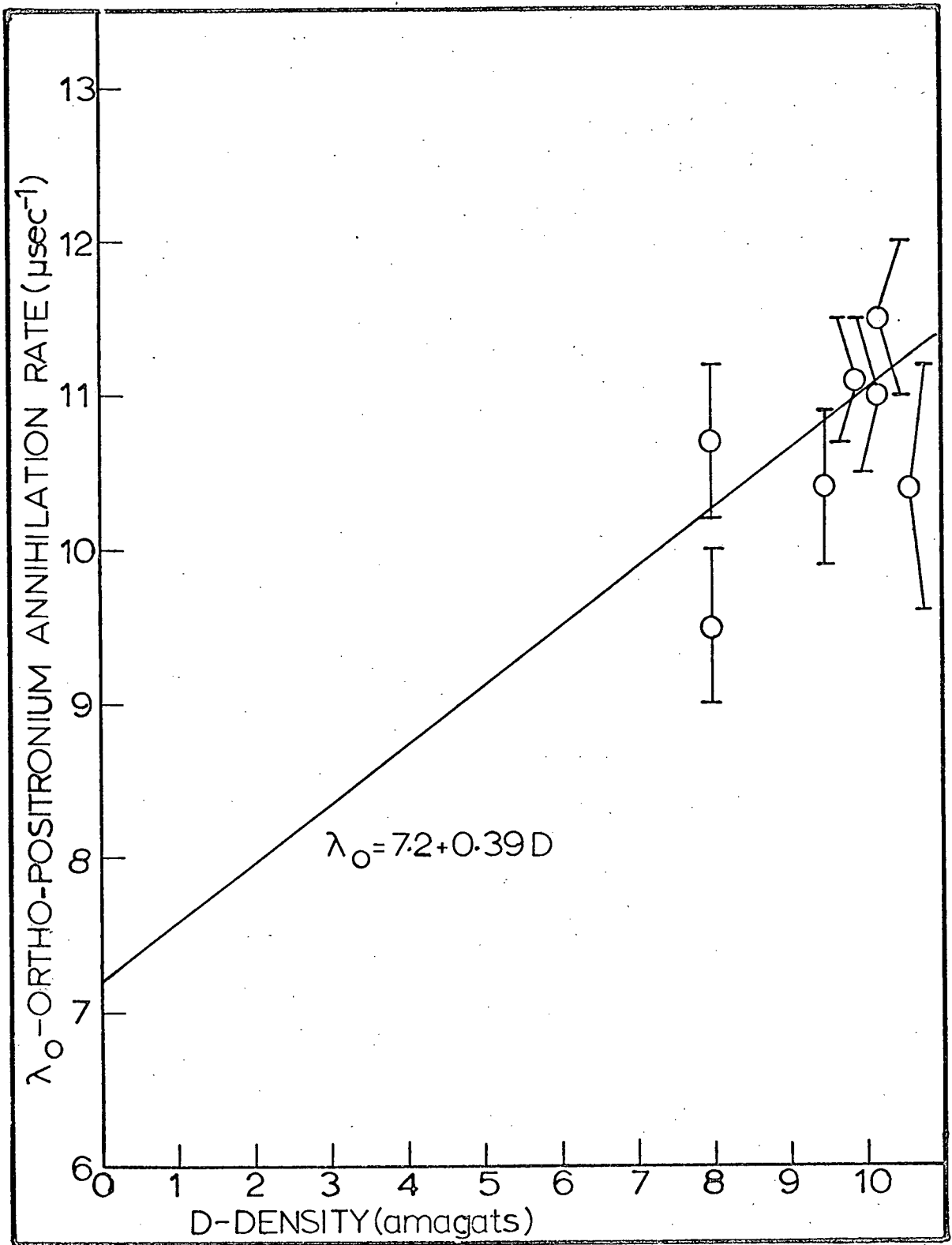


Figure 13: A Graph of the Ortho-positronium Annihilation Rate, λ_0 , Plotted against Density, D.

The results obtained here for λ_q , $0.39 \pm 0.12 \mu\text{sec}^{-1}\text{am}^{-1}$, is much higher than that found by Orth (1966) but the rather large standard deviation on this result bring it within statistical agreement with Orth's result of $0.29 \pm 0.04 \mu\text{sec}^{-1}\text{am}^{-1}$. Although the statistics of this result are rather poor, the quenching rate is large enough to admit the possibility of some minor impurity being present in the gas which affected the ortho-positronium annihilation rate. However, this same impurity should have had an adverse effect on the shoulder, an effect that was not observed. Therefore, due to the poor statistics of the ortho-positronium results no definite conclusions can be made on this point.

5) The Shoulder Width:

The shoulder width was measured by counting the number of channels between the top of the prompt peak and the edge of the shoulder (see Figure 1) by the same technique as used by Falk and Jones (1964). The shoulder width-density product remained constant throughout the experiment with an average value of 353 nsec-am regardless of temperature or density (see Table IV). The standard deviation of these results is 13 nsec-am.

If the annihilations in the shoulder took place at thermal or near thermal velocities, the shoulder width would be as temperature dependent as the direct lifetime. Since the shoulder width remains constant with temperature, then

the shoulder annihilations must take place at much higher velocities (or temperatures) than the thermal velocities used during this experiment. This is in agreement with the interpretation of the shoulder being the result of annihilations of thermalizing positrons (Falk and Jones, 1964).

Tao et al (1963) made the statement that most of the free positrons will be annihilated before being thermalized. However, this and other lifetime experiments show that a fairly large fraction (about 1/3) of the free positrons annihilate after they are thermalized. The statement of Tao et al (1963) is based on the premise that the annihilation rate of free positrons is velocity independent. This experiment, on the contrary, shows that the direct annihilation rate is quite velocity dependent.

E. Calculation of the Direct Annihilation.

Cross-Section from the Results of the Least

Squares Curve Fitting:

In this section a transformation is made between $\lambda_a(T)$, the velocity averaged annihilation rate, and $\mathcal{V}'_a(v)$, the velocity dependent annihilation rate. Then $\mathcal{V}'_a(v)$ will be calculated using the experimentally determined $\lambda_a(T)$. Finally, $\sigma_a(v)$, the annihilation cross section is calculated from $\mathcal{V}'_a(v)$.

For a given $\mathcal{V}'_a(v)$, the velocity averaged annihilation rate is given by

$$\lambda_a = \frac{\int_0^{\infty} \mathcal{I}_a(V) V^2 f(V) dV}{\int_0^{\infty} V^2 f(V) dV} \quad (3)$$

where: V = the positron velocity;

$$f(V) = \exp \left\{ - \int_0^{\infty} \frac{m V dV}{\left(kT + \frac{M}{3} \frac{a^2}{\mathcal{I}_d(V)^2} \right)} \right\};$$

$\mathcal{I}_d(V)$ = the collision rate of positrons with gas molecules;

m = the positron mass;

k = Boltzman's constant;

T = temperature in $^{\circ}\text{K}$;

M = mass of the gas atoms;

a = eE/m = acceleration of a positron in a constant electric field;

e = charge of a positron; and

E = the electric field strength.

The function $f(V)$ is the equilibrium velocity distribution of positrons in a gas assuming that the perturbation of $f(V)$ by the annihilation rate $\mathcal{I}_a(V)$ is negligible. Note that the positronium formation rate is neglected because at thermal equilibrium, with energies averaging 0.025 ev, very few positrons will have enough energy to cross the positronium formation threshold of 8.9 ev.

Assuming that

$$\mathcal{I}_a(V) = A + BV + CV^2 + \dots$$

and that $\mathcal{I}_d(V) =$ a constant, then

$$f(V) = \exp(-V^2/\tau^2)$$

$$\text{where } \tau^2 = \frac{2 (kT + (M/3)a^2/\mathcal{V}_d^2)}{m}. \quad (4)$$

Hence, the average annihilation rate for a partial rate of $(\mathcal{V}_a)_n = A_n V^n$ is given by

$$\begin{aligned} (\lambda_a)_n &= \frac{\int_0^\infty A_n V^{2+n} \exp(-V^2/\tau^2) dV}{\int_0^\infty V^2 \exp(-V^2/\tau^2) dV} \\ &= \frac{2A_n \Gamma(n/2 + 3/2) \tau^n}{\sqrt{\pi}}. \end{aligned}$$

For no electric field

$$(\lambda_a)_n = \frac{2A_n \Gamma(n/2 + 3/2)}{\sqrt{\pi}} \left(\frac{2kT}{m}\right)^{n/2}.$$

Hence, for an annihilation rate written in a series in V , the resulting velocity averaged annihilation rate is a series in \sqrt{T} , that is

$$\lambda_a = a + b \sqrt{T} + c T + \dots$$

From the curve fitting performed earlier the velocity dependent rate can be calculated. For the direct rates reported by equations 1 and 2 in this chapter, the \mathcal{V}_a are as follows:

$$\mathcal{V}_a(V) = 11.9 - 9.23 \times 10^{-7} V + 2.46 \times 10^{-14} V^2 \mu\text{sec}^{-1} \text{ am}^{-1} \quad (5)$$

$$\text{and } \mathcal{V}_a(V) = 1.02 \left(\frac{V_{\text{thr}}}{V}\right)^{0.57} \mu\text{sec}^{-1} \text{ am}^{-1} \quad (6)$$

where $1/2 m V_{\text{thr}}^2 = 8.95 \text{ ev}$, the positronium threshold energy in Argon.

It should be noted that the two entirely different functional relationships, equations 5 and 6, only give meaningful values of

$\mathcal{V}_a(V)$ over the velocity (i.e. temperature)

range investigated.

From the rates $\mathcal{V}_a(V)$ it is a simple matter to calculate the positron annihilation cross section,

$$\sigma_a(V) = \frac{\mathcal{V}_a(V)}{N V}$$

Where: N = the number density of gas atoms.

Hence, for the annihilation rates from equations 5 and 6, the cross sections are:

$$\sigma_a(V) = \left(\frac{5.05 \times 10^3}{V} - 3.90 \times 10^{-4} + 1.04 \times 10^{-11} V \right) \pi a_0^2 \quad (7)$$

$$\text{and } \sigma_a(V) = 2.42 \times 10^{-6} \left(\frac{V_{\text{thr}}}{V} \right)^{1.57} \pi a_0^2 \quad (8)$$

where a_0 = the first Bohr radius.

At 24°C both of these cross sections give $2.41 \times 10^{-4} \pi a_0^2$ for the positron annihilation cross section assuming that $V = \sqrt{2kT/m}$, the most probably velocity at temperature, T .

In comparison with equation 8, the cross sections of Jones et al (1965) from electric field results is $\sigma_a(V) = A/V^{1.42}$ assuming a constant \mathcal{V}_a . As can be seen, these results are quite similar. The difference is thought to arise principally from the fact that Jones et al (1965) did not consider the effect of room temperature when calculating their results. That is, from equation 4, the total effective positron temperature in an electric field, E , is

$$T_{\text{EFF}} = T + \frac{M}{3k} \left(\frac{eE}{M \mathcal{V}_d} \right)^2 \quad (9)$$

This would cause a non-linear dependence in a $\log(E)$ versus $\log(\lambda_a)$ plot, since for low electric fields the temperature

is not negligible, as was assumed by Jones et al (1965).

F. Calculation of the Scattering Cross-Section:

Since the electric field has an effective temperature (see equation 9) of

$$TE = \frac{M}{3k} \left(\frac{eE}{m \mathcal{V}_d} \right)^2, \quad (10)$$

an electric field result of Orth (1966) can be compared with the temperature results obtained in this experiment and get an estimate of \mathcal{V}_d . For $E/D = 14.2$ volts $\text{cm}^{-1}\text{am}^{-1}$, 4.87 was the value of λ_a/D which corresponds to a temperature of 420°K (see Figure 10 or equation 1) or 0.0362 ev. Subtracting room temperature, 24°C or 0.0256 ev, and evaluating equation 10,

\mathcal{V}_d is found to be 9.01×10^{12} collisions/sec at 10 am. This means the cross section,

$$\sigma_d(V) = \frac{\mathcal{V}_d}{NV}, \quad \text{is given by:}$$

$$\sigma_d(V) = 2.14 \left(\frac{V_{\text{thr}}}{V} \right) \pi a_0^2.$$

At 24°C , then, σ_d is $40.0 \pi a_0^2$.

These values were obtained from the results of equations 3 and 4 which used the following assumptions:

1) The distribution function $f(V)$ is Maxwellian, that is $\mathcal{V}_a(V)$ is very much smaller than $\mathcal{V}_d(V)$. ($5.4 \times 10^6 \text{ sec}^{-1}\text{am}^{-1}$ compared to $9.0 \times 10^{11} \text{ sec}^{-1}\text{am}^{-1}$).

2) $\mathcal{V}_d(V)$ is assumed independent of velocity in lieu of a more suitable form.

Finally, since the annihilation rates used in this cal-

culatation (electric field and temperature) are experimental results, this result for ν_d does not depend on the functional form of $\nu_d(V)$.

G. Estimation of Errors:

The pressure gauge used during this experiment was ~~calculated~~ ^{calibrated} against a larger, more accurate gauge ($\frac{1}{2}\%$ of full scale reading, 160 psig full scale) and was found to agree with this standard to within 1 lb between 40 - 160 psig in increments of 15 psig. Also, the estimated error in reading the gauge used was judged to be ± 1 psig. This means the uncertainty in the value of the pressure was less than 3% at 120 psig.

The error in determining the temperature is taken to be $\pm 2\%$ of the difference between room temperature (or ice temperature) and the actual gas temperature. This is essentially the error inherent in the V.T.V.M. Therefore, the uncertainty in temperature at 144°K is 2% and in temperature at 480°K is 1%. During any run the temperature varied by no more than $\pm 3^\circ\text{K}$ from the average temperature of the run. This difference is not larger than the instrumental errors in most cases. Room temperature was determined by an ordinary laboratory thermometer (mercury) to within $\pm 0.2^\circ\text{C}$.

If the chamber did not leak during the run, that is, the density remained constant, then the measured temperature and pressure varied together according to the Ideal Gas

equation to within 1%. A check made by Van der Waals equation indicates that Argon should deviate by 2% from an ideal gas at 143°K and by 1% at 480°K. The total systematic error in density is 4% for any temperature used. Hence, it would seem that Argon should be treated as a perfect gas for this experiment since the measuring equipment is not accurate enough to indicate deviations to the ideal case. This, as has been indicated at the beginning of this paragraph, was what was observed.

The systematic error in the lifetimes due to the integral linearity of the kicksorter is estimated to be 1% (Orth, 1966), leading to a total possible systematic error in λ_e/D of 4%.

CHAPTER VCONCLUSIONS

In this experiment the direct annihilation rate was measured as a function of temperature in Argon gas, between 140°K and 480°K , by the lifetime technique. The direct annihilation rate was found to decrease with increasing temperature. Since the temperature of the gas defines the average velocity of the positron in the gas, then the direct annihilation rate must decrease with increasing velocity at low positron velocities. This is in agreement with the previous results for positrons in Argon with an electric field (Falk et al, 1965).

The shoulder width was found to remain constant with changing temperature indicating that the annihilations taking place in the shoulder occur at velocities significantly higher than thermal velocities.

The statistics on the ortho-positronium annihilation rate were not sufficiently good to notice a temperature dependence of this component.

BIBLIOGRAPHY

- Alcan (1961). "Handbook of Aluminum". Aluminum Company of Canada, Ltd.
- Armstrong, T.N. (1959). "Air Conditioning Refrigerating Data Book, Refrigeration Applications". American Society of Heating Refrigerating and Air-Conditioning Engineers Inc.
- ASME Boiler and Pressure Vessel Code (1965). The American Society of Mechanical Engineers.
- Celitans, G.J. and Green, J.H. (1963). Proc. Phys. Soc. 82, 1002.
- Deutsch, M. (1953) Progr. Nucl. Phys. 3, 131.
- Du Mond, T.C. (1951). "Engineering Materials Manuel". Reinhold Publishing Corp.
- Falk, W.R. (1965). Ph. D. Thesis, University of British Columbia.
- Falk, W.R. and Jones, G. (1964). Can. J. Phys. 42, 1751.
- Falk, W.R., Orth, P.H.R., and Jones, G. (1965). Phys. Rev. Letters 14, 447.
- Handbook of Chemistry and Physics, 47th. Edition (1965). Chemical Rubber Publishing Co.
- Jones, G. Falk, W.R., and Orth, P.H.R. (1965). Paper presented at the IVth International Conference of the Physics of Electronic and Atomic Collisions (1965).
- Jones, G. and Orth, P.H.R. (1967). "Positron Annihilation" (A.T. Stewart and L.O. Roellig, ed.). Academic Press, N.Y.
- Orth, P.H.R. (1967). Ph. D. Thesis, University of British Columbia.
- Paul, D.A.L. (1964). Proc. Phys. Soc. 84, 563.

Paul, D.A.L. and Graham, R.L. (1957). Phys. Rev. 106, 16.

Roellig, L.O. and Kelly, T.M. (1965). Phys. Rev. Letters
15. 746.

Superior Tube Catalogue 23 (1965). Superior Tube Co.

Tao, S.J. and Bell, J. (1967). "Positron Annihilation"
(A.T. Stewart and L.O. Roellig, ed.). Academic Press,
N.Y.

Tao, S.J., Bell, J., and Green, J.H. (1964). Proc. Phys.
Soc. 83, 453.

Tao, S.J., Green, J.H. and Celitans, G.J. (1963) Proc.
Phys. Soc. 81, 1091.

Timoshenko, S. (1956). "Strength of Materials, Part II"
(3rd. edition). D. Van Nostrand Company, Inc., N.J.

APPENDIXCALCULATION OF THE LONGITUDINAL STRESS IN
THE FLANGE OF THE CHAMBER

The longitudinal stress in the chamber wall at the joint between the cylinder wall and the flange is given by

$$(1) \quad s = \frac{6M_o}{h_1^2} + \frac{pc}{2h_1}$$

where M_o is determined by solving the following simultaneous equations from Timoshenko (1956), as pictured in Figure 14:

$$(2) \quad y = \frac{1}{2B^3 D} (P_o - BM_o) \quad (\text{Eqn. 11});$$

$$(3) \quad \Theta = \frac{1}{2B^2 D} (P_o - 2BM_o) \quad (\text{Eqn. 12});$$

$$(4) \quad y = y_1 - y_2 = \frac{pc^2(2-u)}{2h_1 E} - \frac{h}{2} \Theta \quad (\text{Page 125});$$

$$(5) \quad M_t = c/a [R(d-c) + M_o + P_o h/2] \quad (\text{Page 142});$$

$$(6) \quad \text{and } \Theta = \frac{12 M_t a}{Eh^3 \ln(d/c)} \quad (\text{Eqn. 128});$$

$$\text{where: } D = \frac{Eh_1^3}{12(1-u^2)} ;$$

$$B = \left[\frac{3(1-u^2)}{c^2 h_1^2} \right]^{1/4} ;$$

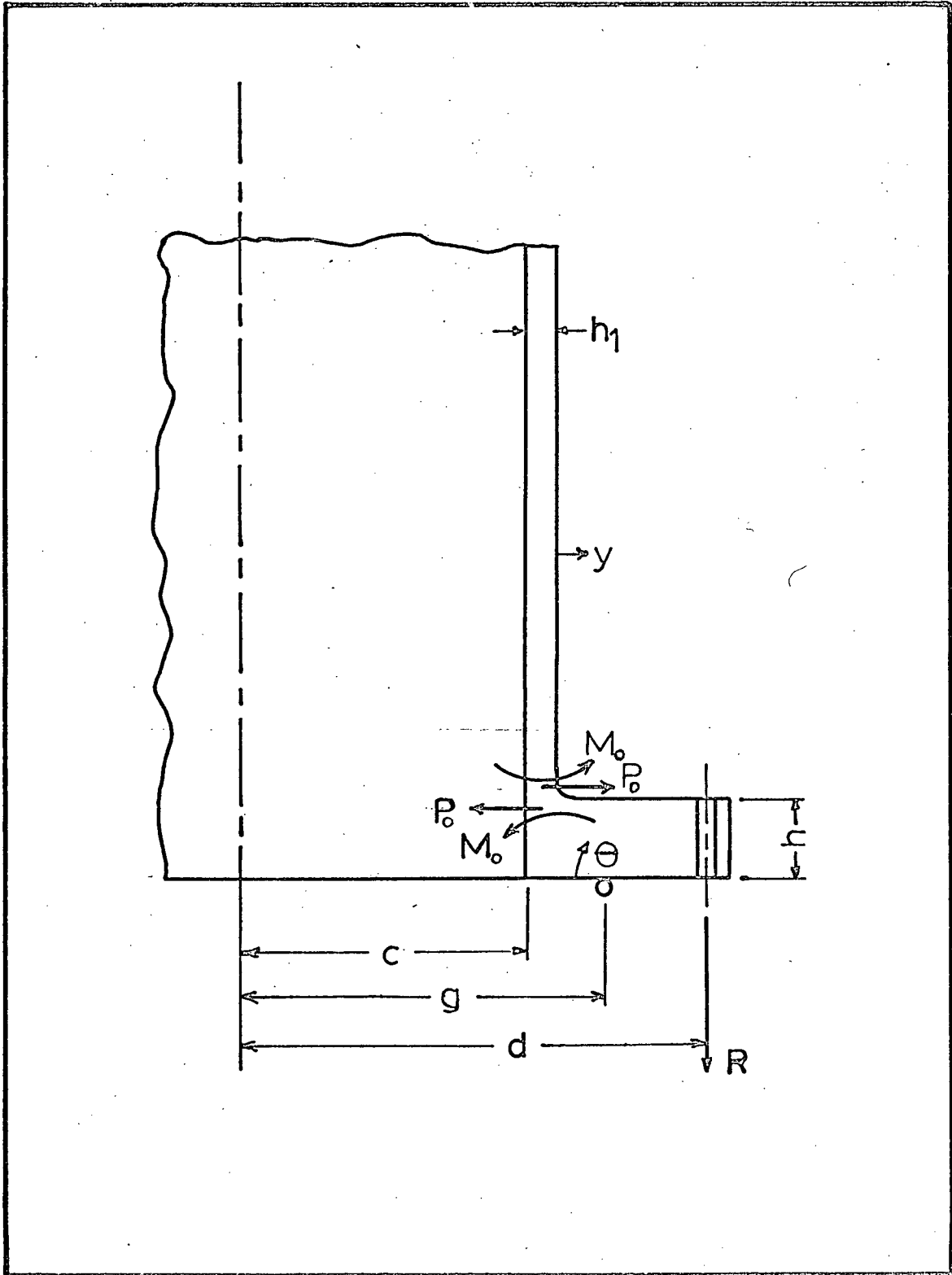


Figure 14: A diagram Showing Forces and Moments on the Flange.

- c = inner radius of the cylinder = 3.03 in.;
 d = radius of bolt circle = 4.125 in.;
 a = $\frac{1}{2} (c + d)$;
 h = thickness of flange = 0.9 in.;
 h_1 = thickness of chamber wall = 0.28 in.;
 y = deflection of chamber wall due to pressure load (y_1) and flange rotation ($-y_2$);
 Θ = angle of flange rotation;
 p = pressure in psi;
 M_0 = bending moment per length at the flange-wall junction;
 P_0 = shearing force at the flange-wall junction;
 u = Poisson's ratio = 0.33;
 E = Young's modulus;
 M_t = bending moment per length of the flange at its center point;
 R = bolt load per length due to pressure in the vessel = $g^2 p / 2c$; and
 g = radius of "O" ring gasket = 3.375 in.

When the values of the various parameters are placed into equations 2-6, they can be solved simultaneously for M_0 in terms of p . If the resulting $M_0 (p)$ is placed into equation 1, equation 1 can be solved for the maximum allowable p with S placed equal to the maximum allowable stress of 14,900 psi in Stainless Steel at 300°C.

This calculation shows that the maximum allowable pressure for a safe flange is 950 psi.